Tetrahedron Green Chem 1 (2023) 100011

Contents lists available at ScienceDirect

Tetrahedron Green Chem

journal homepage: www.journals.elsevier.com/tetrahedron-green-chem

Piperazine-Amberlyst®15-catalysed synthesis of 2-amino-4*H*-chromenes, chromeno[2,3-*b*]pyridines and chromeno[2,3-*d*]pyrimidines

Giovanna Bosica *, Roderick Abdilla

Green Synthetic Organic Chemistry Lab, Department of Chemistry, University of Malta, Msida, Malta

ARTICLE INFO

Keywords:
2-Amino-4H-chromenes
chromeno[2,3-*b*]pyridines
chromeno[2,3-*d*]pyrimidines
Piperazine-Amberlyst® 15
Heterogeneous catalyst
Multicomponent reactions
Green
Recyclable
Cheap

ABSTRACT

Chromenes, biologically-active scaffolds, and their variants have been often synthesized by the combination of salicylaldehyde, malononitrile, and nucleophilic species (indoles, naphthols, nitro compounds, thiols). Whereas this combination furnishes specifically 2-amino-4*H*-chromenes, other related compounds such as chromeno[2,3-*b*]pyridines and chromeno[2,3-*d*]pyrimidines may be also attained using similar readily available reactants: salicylaldehyde, two equivalents of malononitrile and a thiol for the former and malononitrile, two salicylaldehyde equivalents and an amine for the latter. To the best of our knowledge, there are no reported studies which have attempted to synthesize these products using the same catalyst. Hence, the aim of the below study was to find a cheap and recyclable catalyst that would be able to drive the synthesis of all three products. Positively, piperazine supported on the polymeric sulfonic acid resin Amberlyst® 15 was found to be an inexpensive and easily-prepared novel catalyst that could be used to synthesize all three derivatives (33 examples, 18–82%) in fairly good yields whilst also being recyclable and reusable (for up to four or five runs).

1. Introduction

Multicomponent reactions involve the combination of three or more reactants in the same reaction-pot and often yield complex heterocycles such as pyridines, pyrimidines, pyrazolines, imidazoles, furans and chromenes amongst others [1–4]. 2*H*/4*H*-Chromenes (polycyclic oxygen heterocycles comprising an aryl ring system fused at a 5,6-positioned pyran ring) are a versatile biological scaffold that were found to be attractive due to their antimicrobial activity (Fig. 1, structures A - C) [4]. Furthermore, it was also discovered that substitutions on the 2nd, 3rd and 4th positions of 4-aryl-4*H*-chromenes led to species with enhanced antitumor activity which was further reinforced if the aryl component had halogen substituents at the 3rd position (Fig. 1, structure D) [5,6].

Chromene scaffolds have been synthesized via an array of methods such as via the reaction between aldehydes, an activated methylene compound and a naphthol/phenol. Amongst the broad number of base and acid-catalysed studies, ZrO_2, NiO_2, piperazine-graphene oxide and prolinamide-functionalized polyacrylonitrile have all been utilised to varying degrees of success [7–10]. An alternative reaction (Scheme 1) with a greater room for diversity and which furnishes 4-substituted-2-amino-3-cyano-4*H*-chromenes (**9a-e,** Scheme 1**)** involves the combination of an activated methylene compound such as malononitrile (**1a**), salicylaldehyde (**2a**) (which acts as an aldehyde and as phenol simultaneously) and a nucleophilic reagent such as thiophenol (**3a**), 2-methylindole (**4a**), nitromethane (**5**), 2-naphthol (**6**) and hydrazine (**7**) in tandem with methyl acetoacetate (**8**) *etc.* [11–17]. Although the range of catalysts which has been explored for these reactions is also significantly broad, usually studies limit themselves to one or few nucleophile types: thiophenol [11,12], nitromethane [13,14], 2-naphthol [15], indoles [16] and dimedone [17]. In truth, in the study by Ghosh, P. et al., where nano-zinc oxide was the catalytic agent, diverse nucleophiles were tried including: indole, 4-hydroxycoumarin and 4-aminocoumarin amongst others [15]. Yet, nano-zinc oxide, being non-magnetic, renders recovery more troublesome especially on an industrial scale where specific filters would have to be used.

Interestingly, the reaction between salicylaldehyde (**2a**), malononitrile (**1a**) and thiophenol (**3a**) can be extended further by using two equivalents of malononitrile (instead of one) to furnish chromeno[2,3-*b*]pyridines (Scheme 2) as attested by studies employing K_2CO_3 [18], ZrP_2O_7 [19], SnO [20] and chitosan-citric acid [21] as heterogeneous catalysts (K_2CO_3 is actually a homogeneous catalyst).

Looking further into the chemistry of salicylaldehyde-derived chromenes, there have been various reports about the pseudo-4-component reaction between malononitrile (**1a**), two equivalents of

* Corresponding author.
E-mail address: giovanna.bosica@um.edu.mt (G. Bosica).

https://doi.org/10.1016/j.tgchem.2023.100011
Received 23 March 2023; Received in revised form 3 May 2023; Accepted 9 May 2023
Available online 12 May 2023

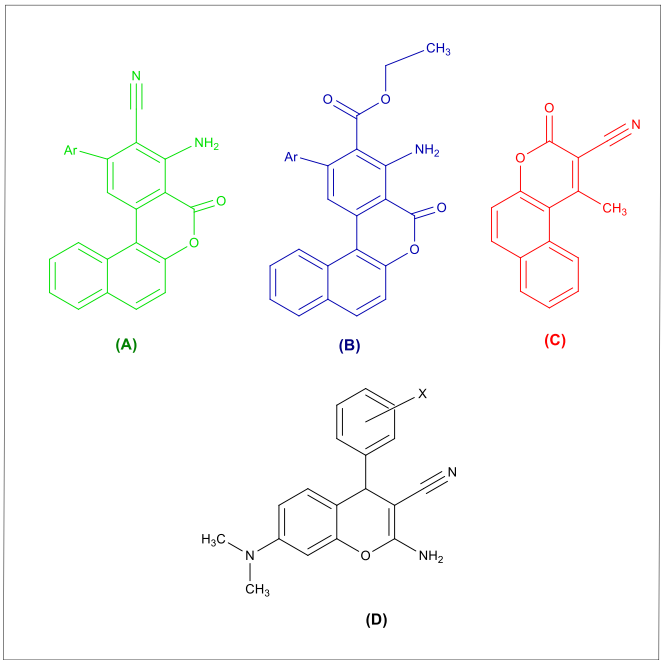

Fig. 1. Dibenzochromenes with biological activity [4,5].

salicylaldehyde (**2a**), and a secondary amine (**11**) in order to synthesize chromeno[2,3-*d*]pyrimidines (**12**) (Scheme 3) [21–30]. Various catalysts have been developed to drive the reaction usually in short reaction times and in neat conditions including: aminopropyl-grafted magnetite [22], manganese(III) salen complex immobilized on magnetite [23], nano-zinc aluminate [24], polystyrene sulfonic acid [25], 2-aminoethyl-3-propylimidazolium bromide supported on Santa Barbara Amorphous silica 15 (SBA-15) [26], phosphomolybdic acid supported on creatin halloysite clay [27], nano-silver xerogel [28], titania-silica [29] and sulfamic-acid functionalized magnetic isoreticular metal organic framework-3 (IRMOF-3) nanocomposite [30].

Albeit the fact that most of these catalysts furnish the products in excellent yields in short reaction times, most catalyst preparations require quite elaborate and lengthy procedures which necessitate harmful solvents such as toluene or dichloromethane and, in some cases, also require expensive starting materials. In addition, to the best of our knowledge, there has not been any study which attempted to synthesize 4*H*-chromenes, chromeno[2,3-*b*]pyridines and chromeno[2,3-*d*]pyrimidines using the same catalyst. In the below study, this has been achieved using the novel catalyst piperazine supported on Amberlyst® 15 (Pip-A15), which is relatively simple to prepare and cheap.

2. Experimental

2.1. General reaction procedures

2.1.1. Synthesis of 4-substituted 2-amino-3-cyanochromenes (9a-e)

To a nitrogen-flushed dry 25-mL-two-necked flask, malononitrile (2.5 mmol) and salicylaldehyde (2.5 mmol) were added in that order followed by a few drops of ethanol (0.5 mL) and the catalyst. The mixture was left to stir for approximately 10 min at room temperature before addition of 2-naphthol, nitromethane, 2-methylindole or thiophenol (2,5 mmol of either of them) and further ethanol solvent (3.5 mL) and then heating to the required temperature. The reaction was monitored using TLC or GC at 0.5–1 h intervals and was stopped until complete consumption of the latter added reagent or until no further change was observed. Subsequently, the reaction mixture was dissolved in hot acetone, filtered using a G4 funnel and then concentrated under vacuum by rotary evaporation. The crude solid was recrystallized from ethanol or ethanol/water (8:2).

2.1.2. Synthesis of benzopyrano[2,3-b]pyridines (10a-h)

To a nitrogen-flushed dry 25-mL-two-necked flask, malononitrile (5.0 mmol) and salicylaldehyde (2.5 mmol) were added in that order followed by a few drops of ethanol (0.5 mL) and the catalyst. The mixture was left to stir for approximately 10 min at room temperature before addition of 2-thiophenol (2.5 mmol) and further ethanol solvent (3.5 mL) and then heating to the required temperature. The reaction was monitored using TLC at 1 h intervals and was stopped until complete consumption of thiophenol or until no further change was observed. Subsequently, the reaction mixture was dissolved in DMF (7 mL), filtered using a G4 funnel and then concentrated under vacuum by rotary evaporation set at 40 °C/-1 bar. Subsequently, deionised water (10 mL) was added and the product precipitated out. In order to ensure further precipitation, the flask was left to cool in the fridge overnight before filtering, drying and collecting the product. In some cases the product was stirred in hot methanol (10–20 mL) to remove any adsorbed thiophenol or side products.

2.1.3. Synthesis of benzopyrano[2,3-d]pyrimidines (12a-i)

To a nitrogen-flushed dry 25-mL-two-necked flask, malononitrile (2.5 mmol) and salicylaldehyde (5.0 mmol) were added in that order followed by a few drops of methanol solvent (0.5 mL) and the catalyst. The mixture was left to stir for approximately 10 min at room temperature before addition of further solvent (3.5 mL), the amine (2.5 mmol) and then heating to the required temperature. The reaction was monitored using TLC at 1-h intervals and was stopped until complete consumption of the salicylaldehyde (visible under short wavelength UV). Subsequently, the reaction mixture was dissolved in hot ethanol, filtered and then concentrated under vacuum by rotary evaporation set at 45 °C/-1 bar. The crude solid was then recrystallized from ethanol.

2.2. Catalyst synthesis

2.2.1. Piperazine/DABCO/DBU/Ethylenediamine (EDA)/DMAP supported on Amberlyst® 15 (Pip/DABCO/EDA/DMAP-A15)

For the preparation of Piperazine supported on Amberlyst® 15 (Pip-A15-A), to a nitrogen-flushed dry 50-mL single-necked flask, Amberlyst® 15 beads (0.6 g), previously dried at 100 °C in an air-oven for 12 h, were added followed by 1–2 mL of ethanol solvent. Subsequently, piperazine (0.4 g) was added in portions to the flask. The mixture was left to stir for 48 h at RT after which it was filtered through a G4 Hirsch funnel. The solid filtered catalyst beads were heated further for 12 h at 100 °C before noting the mass difference compared to that of the originally weighed Amberlyst® 15 beads. Finally, the catalyst was transferred to a pestle and mortar and ground into a fine powder. The same procedure was followed in the preparation of other amines supported on Amberlyst® 15 using either: DABCO, DBU, ethylenediamine or DMAP.

In the preparation of Pip-A15-B, the filtered catalyst after 48 h of stirring was heated at 120 °C under vacuum before noting mass difference (for determination of loading) and then grinding to a fine powder. For the preparation of Pip-A15-C, Amberlyst® 15 beads (0.6 g) and piperazine (0.4 g) were refluxed in ethanol (10 mL) whereas for Pip-A15-D 7 : 3 ethanol/water was used (10 mL) and for Pip-A15-E, the solvent used was acetonitrile (10 mL). Pip-A15-F was prepared by first crushing the previously dried Amberlyst® 15 beads (0.6 g) and then refluxing (along with piperazine, 0.4 g) in acetonitrile (10 mL). Pip-A15-G was prepared like Pip-A15-E but using 0.15 g piperazine and 0.85 g Amberlyst® 15 beads.

Alkalinity of the prepared catalysts was determined as follows.

The final dry and crushed prepared catalyst (Pip-A15-A,B,C,D or E) was stirred (0.05 g) in 10 mL aqueous hydrochloric acid (0.02 M) for 2 h at room temperature in a 50-mL round-bottomed single-neck flask fitted with a cap. Subsequently, catalyst was filtered, washed with deionised

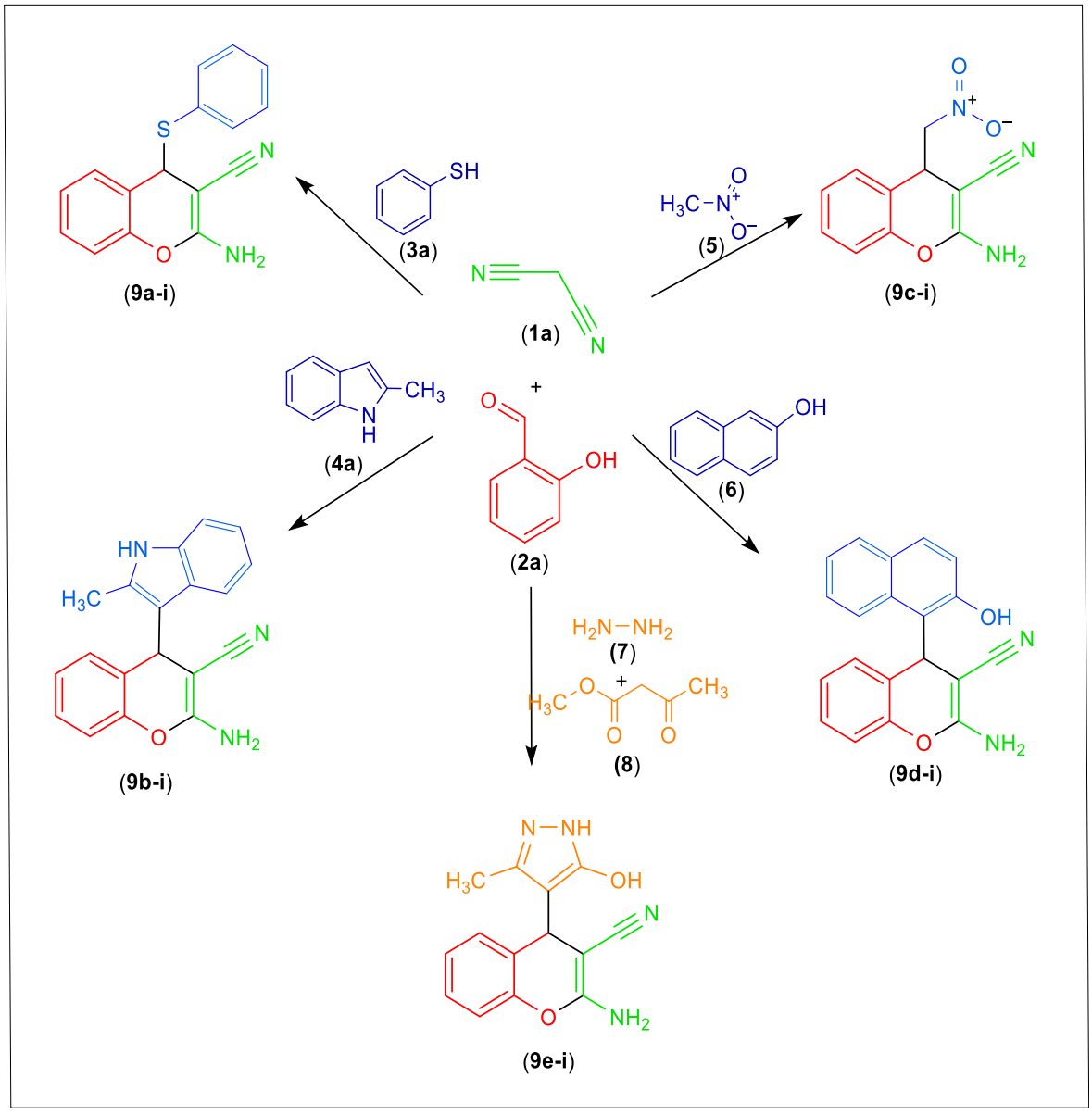

Scheme 1. Synthesis of 4-substituted 2-amino-3-cyano-4*H*-chromenes (**9a-i**) from malononitrile (**1a**), salicylaldehyde (**2a**) and nucleophilic reagents such as thiophenol (**3a**), 2-methylindole (**4a**), nitromethane (**5**), 2-naphthol (**6**), and hydrazine (**7**) in combination with methyl acetoacetate (**8**).

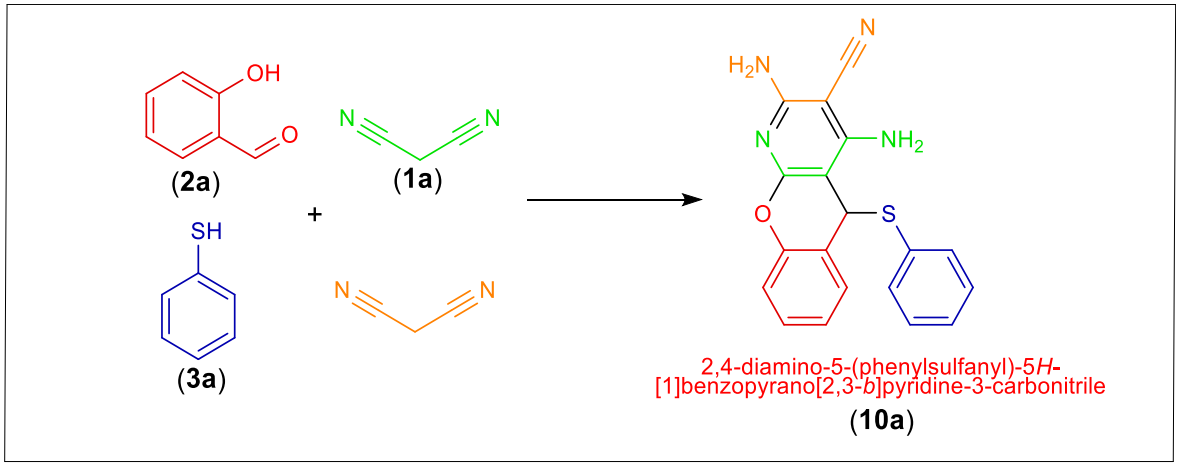

Scheme 2. Pseudo 4-component synthesis of benzopyrano[2,3-*b*]pyridines (**10a**) from malononitrile (**1a**), salicylaldehyde (**2a**) and thiophenol (**3a**).

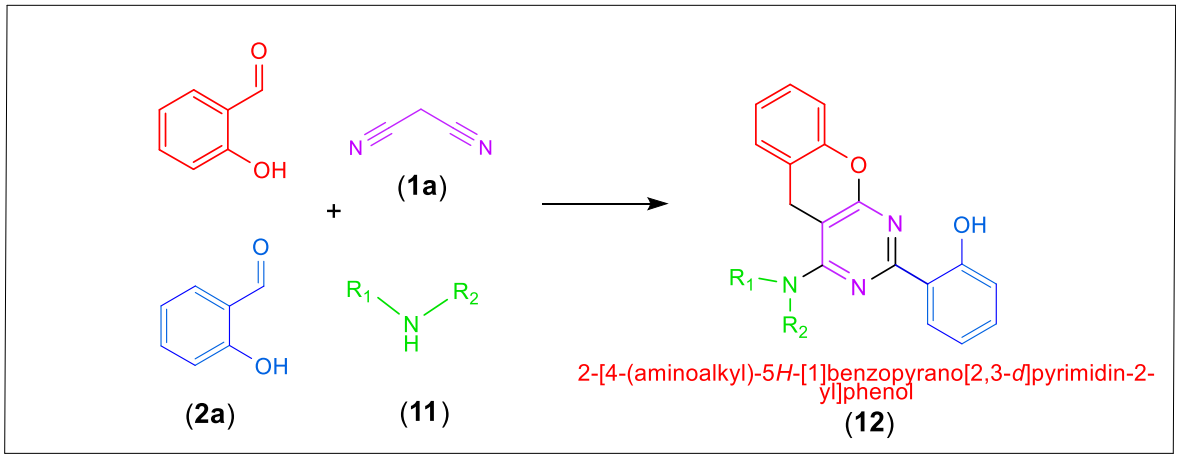

Scheme 3. Pseudo-4-component synthesis of benzopyrano[2,3-*d*]pyrimidines (**12**) using two equivalents of salicylaldehyde (**2a**), malononitrile (**1a**) and a secondary amine (**11**).

water (3 × 10 mL) before titrating the filtrate with aqueous sodium hydroxide (0.02 M) using 10% w/v alcoholic phenolphthalein solution as an indicator to a slightly-pink end-point.

For comparison, the acidity of unsupported Amberlyst® 15 beads was determined as follows.

Previously dried (at 100 °C for 12 h) Amberlyst® 15 beads were ground and then 0.05 g of the resulting powder was stirred with aqueous sodium hydroxide (10 mL, 0.02 M) for 2 h, filtered, washed with deionised water (3 × 10 mL) and then the filtrate was titrated with aqueous hydrochloric acid (0.02 M) using the same indicator to a colourless end point.

2.2.2. Piperazine/DABCO/DBU supported on chloropropylsilylated silica (Pip-SiO_2, DABCO-SiO_2. DBU-SiO_2 [31,32]

The method is a slightly modified version of that suggested by Hasaninejad, A. et al. [31,32] Silica (25 g) was first immersed in 6 M hydrochloric acid for 24 h and then washed repeatedly with water before drying under vacuum and then in an oven at 120 °C for 24 h. The final product is termed as activated silica.

A mixture of dry toluene (30 mL) and activated silica (2.5 g) was refluxed for 48 h after addition of 3-chloropropyltrimethoxysilane (2.5 mL) and triethyl amine (0.25 mL). The chloropropylsilylated silica was then filtered, washed with toluene (30 mL) and with acetone (30 mL) before leaving to dry in desiccator for 24 h. The final product is termed as chloropropylsilylated silica.

Subsequently, DABCO, piperazine or DBU (5 mmol) were added to the chloropropylsilylated silica (1.0 g) in 30 mL of dry acetone and the latter mixture was refluxed for 36 further hours before filtering, washing with further acetone and then leaving to dry in desiccator. For the preparation of DBU-SiO_2 the solvent used was cyclohexane instead of acetone.

CaO supported on dolomite was prepared by following the reported procedure [33], KF-alumina was prepared as per procedure [34], KF-Zeolite was prepared according to Ref. [35], MgO was prepared according to Ref. [36], SnO_2 was synthesized based on method in Ref. [37], CaO was prepared according to method in Ref. [38], Chit-NH_2 was synthesized as per [39], ZrO_2–NH_2 and Cell-NH_2 were synthesized by following the same method reported for silica [40] but replacing the latter with zirconia/microcrystalline cellulose, K_2CO_3–SiO_2 was formed by following method [41], sulfated zirconia/alumina was prepared as per reported method [42], methane sulfonic acid supported on alumina was synthesized based on [43], PW/Wsi on MK30/Al_2O_3 was synthesized by following the same method provided in Ref. [44], silica-bonded DABCO hydrogen sulfate was synthesized as per [45], CuI-A21 was synthesized as per [46] whilst A26 was dried by following the same procedure reported in the same publication for A21.

2.3. Product characterization procedure

IR spectra were recorded on a Shimadzu IRAffinity-1 FTIR spectrometer calibrated against 1602 cm-1 polystyrene absorbance spectra. Samples were analysed as a KBr pellet after carrying out a background scan using KBr only. The pellets were prepared by grinding about 5–10 mg of each separate sample with 100 mg of oven-dried potassium bromide with a pestle and mortar before subjecting them to pressure in a screwable die. The final spectra were given as % transmittance against wavenumber (cm^{-1}) and could be analysed and processed by the software Irsolution® before exporting as.txt files and then opening in MS Office Excel®. The NMR spectra were recorded on a Bruker Avance III HD® NMR spectrometer, equipped with an Ascend 500 11.75 T superconducting magnet, operating at 500.13 MHz for ^{1}H and 125.76 MHz for ^{13}C, and a multinuclear 5 mm PABBO probe. Samples were dissolved in deuterated chloroform, DMSO or acetone (with TMS). For ^{1}H NMR, the product (3–5 mg) was dissolved in 0.8 mL of deuterated solvent whilst for ^{13}C NMR the mass of product (dissolved in the same volume) was increased to 30–50 mg. The NMR spectra were analysed and processed by Topspin Software, ver. 3.2® and by MestreNova®. Mass spectra were performed using a Waters Acquity® TQD system equipped with a tandem quadrupole mass spectrometer and analysed directly with a probe. The spectra were obtained in relative abundance against *m/z* and were generated by the software MassLynx®. Melting point determination of products was carried out using a Stuart® SMP11 melting point determination apparatus fitted with a mercury thermometer. Three separate readings were taken and the mean average was then calculated for better accuracy.

2.3.1. Analytical data

[9a-i] 2-amino-4-(phenylsulfanyl)-4*H*-1-benzopyran-3-carbonitrile [11]**.** Yellow solid. IR (KBr) (ν_{max}, cm^{-1}): 3433, 3321, 3233, 3202, 3075, 3055, 2201, 1655, 1605, 1489, 1416, 1265, 1219, 1190, 1067, 1042, 1026, 891, 775, 762, 704, 691, 638, 602. ^{1}H NMR (500 MHz, DMSO-d_6) δ 7.37–7.29 (m, 2H), 7.26–7.19 (m, 3H), 7.16 (td, J = 7.4, 1.3 Hz, 1H), 7.07–7.00 (m, 4H), 6.79 (dd, J = 8.1, 1.2 Hz, 1H), 5.34 (s, 1H).

[9a-ii] 2-amino-7-bromo-4-(phenylsulfanyl)-4*H*-1-benzopyran-3-carbonitrile [11]. Yellow solid. IR (KBr) (ν_{max}, cm^{-1}): 3455, 3333, 3275, 3071, 2201, 1651, 1603, 1568, 1476, 1418, 1267, 1223, 1180, 1024, 822, 735, 694. ^{1}H NMR (500 MHz, Acetone-d_6) δ 7.52 (dd, J = 2.4, 0.6 Hz, 1H), 7.42–7.37 (m, 2H), 7.30–7.25 (m, 2H), 7.17–7.13 (m, 2H), 6.76 (d, J = 8.7 Hz, 1H), 6.34 (s, 2H), 5.23 (s, 1H).

[9a-iv] 2-amino-7-nitro-4-(phenylsulfanyl)-4*H*-1-benzopyran-3-carbonitrile [11]. Yellow solid. IR (KBr) (ν_{max}, cm^{-1}): 3447, 3420, 3327, 3204, 3078, 2201, 1651, 1531, 1520, 1410, 1348, 1260, 1238, 1188,

1082, 824,745, 700. ^{1}H NMR (500 MHz, Acetone-d_6) δ 8.32 (dd, J = 2.8, 0.6 Hz, 1H), 8.13 (dd, J = 9.1, 2.8 Hz, 1H), 7.40 (ddt, J = 8.7, 7.0, 1.3 Hz, 1H), 7.29–7.24 (m, 2H), 7.17–7.13 (m, 2H), 7.01 (d, J = 9.1 Hz, 1H), 6.51 (s, 2H), 5.41 (s, 1H).

[9a-v] 2-amino-4-[(4-methylphenyl)sulfanyl]-6-nitro-4*H*-1-benzopyran-3-carbonitrile [NOVEL]. White solid. M.P. = 174 °C. IR (KBr) (ν_{max}, cm^{-1}): 3460, 3323, 3211, 3082, 2205, 1655, 1533, 1481, 1410, 1342, 1261, 1233, 1192, 1084, 1038, 916, 835, 812, 746, 691, 652. ^{1}H NMR (500 MHz, Acetone-d_6) δ 8.29 (dd, J = 2.6, 0.7 Hz, 1H), 8.12 (dd, J = 9.0, 2.6 Hz, 1H), 7.08 (d, J = 7.6 Hz, 2H), 7.04–7.00 (m, 3H), 6.50 (s, 2H), 5.33 (s, 1H), 2.32 (s, 3H). ^{13}C NMR (126 MHz, Acetone-d_6) δ 161.33, 153.42, 144.38, 139.61, 136.80, 129.43, 126.52, 125.18, 123.82, 123.19, 118.00, 116.91, 55.76, 46.13, 20.34. ES(+) m/z = 340.32, 216.83, 169.77, 124.72.

[9b-i] 2-amino-4-(2-methyl-1*H*-indol-3-yl)-4*H*-1-benzopyran-3-carbonitrile [47]. Off-white solid. M.P. = 189 °C. IR (KBr) (ν_{max}, cm^{-1}): 3445, 3343, 3196, 3167, 2974, 2907, 2189, 1651, 1580, 1485, 1456, 1393, 1261, 1227, 1184, 1045, 1015, 768, 750, 669, 627. ^{1}H NMR (500 MHz, DMSO-d_6) δ 10.84 (s, 1H), 7.23 (d, J = 8.0 Hz, 1H), 7.20 (ddd, J = 8.5, 7.1, 1.2 Hz, 1H), 7.06 (dd, J = 8.3, 1.2 Hz, 1H), 7.00–6.97 (m, 2H), 6.96–6.91 (m, 2H), 6.78 (ddd, J = 8.0, 7.0, 1.0 Hz, 1H), 6.74 (s, 2H), 5.07 (s, 1H), 2.45 (s, 3H).

[9b-ii] 2-amino-4-(1*H*-indol-3-yl)-4*H*-1-benzopyran-3-carbonitrile [47]. Yellow solid. M.P. = 204 °C. IR (KBr) (ν_{max}, cm^{-1}): 3451, 3335, 3211, 2191, 1655, 1584, 1491, 1427, 1379, 1277, 1225, 1049, 1005, 957, 922, 760, 687, 627, 600. ^{1}H NMR (500 MHz, Chloroform-*d*) δ 8.07 (s, 1H), 7.39–7.33 (m, 2H), 7.23–7.15 (m, 3H), 7.13 (dt, J = 7.5, 1.3 Hz, 1H), 7.06 (dd, J = 8.3, 1.3 Hz, 1H), 7.05–7.03 (m, 1H), 7.02–6.99 (m, 1H), 5.09 (s, 1H), 4.58 (s, 2H).

[9b-iii] 2-amino-7-bromo-4-(2-methyl-1*H*-indol-3-yl)-4*H*-1-benzopyran-3-carbonitrile [47]. White solid. IR (KBr) (ν_{max}, cm^{-1}): 3451, 3316, 3196, 3055, 2914, 2193, 1651, 1605, 1574, 1477, 1462, 1398, 1296, 1260, 1256, 1225, 1175, 1115, 1038, 1018, 814, 741. ^{1}H NMR (500 MHz, Acetone-d_6) δ 10.03 (s, 1H), 7.38 (dd, J = 8.8, 2.4 Hz, 1H), 7.29 (d, J = 8.2 Hz, 1H), 7.16 (d, J = 2.4 Hz, 1H), 7.14 (d, J = 8.8 Hz, 1H), 7.06 (dd, J = 8.0, 1.3 Hz, 1H), 6.98 (ddd, J = 8.2, 7.0, 1.2 Hz, 1H), 6.84 (ddd, J = 8.0, 7.0, 1.2 Hz, 1H), 6.08 (s, 2H), 5.19 (s, 1H), 2.57 (s, 3H). ^{13}C NMR (126 MHz, Chloroform-*d*) δ 168.44, 161.79, 149.05, 131.96, 130.94, 123.93, 118.06, 117.43, 80.70, 72.37, 51.33, 34.01.

[9b-v] 2-amino-4-(5-bromo-2-methyl-1*H*-indol-3-yl)-7-chloro-4*H*-1-benzopyran-3-carbonitrile [30]. Yellow solid. M.P. = 206 °C. IR (KBr) (ν_{max}, cm^{-1}): 3451, 3408, 3329, 3217, 2195, 1699, 1670, 1651, 1611, 1576, 1481, 1456, 1408, 1260, 1227, 1179, 1096, 818, 800. ^{1}H NMR (500 MHz, Acetone-d_6) δ 10.42 (s, 1H), 7.53 (d, J = 1.6 Hz, 1H), 7.50 (d, J = 2.6 Hz, 1H), 7.39 (dd, J = 8.6, 0.6 Hz, 1H), 7.27 (ddd, J = 8.7, 2.6, 0.6 Hz, 1H), 7.21 (dd, J = 8.6, 1.9 Hz, 1H), 7.16 (dd, J = 2.6, 0.9 Hz, 1H), 7.14 (d, J = 8.7 Hz, 1H), 6.22 (s, 2H), 5.13 (s, 1H). ^{13}C NMR (126 MHz, Acetone-d$_6$) δ 159.78, 147.66, 136.15, 128.94, 128.90, 128.06, 127.38, 125.58, 125.05, 124.26, 121.07, 119.13, 118.27, 117.89, 113.64, 111.97, 58.09, 32.74.

[9b-vi] Methyl 2-amino-4-(2-methyl-1*H*-indol-3-yl)-4*H*-1-benzopyran-3-carboxylate [NOVEL]. Yellow solid. M.P. = 180 °C. IR (KBr) (ν_{max}, cm^{-1}): 3426, 3385, 3304, 3046, 2992, 2947, 2882, 1670, 1609, 1585, 1518, 1485, 1456, 1435, 1383, 1315, 1229, 1188, 1090, 1045, 802, 777, 750, 619, 608. ^{1}H NMR (500 MHz, Chloroform-*d*) δ 7.68 (s, 1H), 7.39 (dd, J = 7.9, 1.1 Hz, 1H), 7.21 (dt, J = 7.9, 0.9 Hz, 1H), 7.11 (ddt, J = 9.0, 5.6, 1.8 Hz, 1H), 7.08–7.02 (m, 4H), 6.99–6.92 (m, 2H), 6.48–6.14 (m, 2H), 5.30 (s, 1H), 3.60 (s, 3H), 2.53 (s, 3H). ^{13}C NMR (126 MHz, Acetone-d_6) δ 169.55, 160.62, 135.74, 130.81, 129.72, 127.18, 127.04, 126.61, 124.14, 119.91, 118.32, 117.89, 117.36, 115.35, 110.24, 49.86, 30.49, 10.84. ES(+) m/z = 335.21, 303.21, 204.10, 172.10.

[9c-i] 2-amino-4-(nitromethyl)-4*H*-1-benzopyran-3-carbonitrile [13]. Orange solid. IR (KBr) (ν_{max}, cm^{-1}): 3451, 3335, 3211, 2191, 1655, 1584, 1533, 1491, 1427, 1379, 1277, 1225, 1049, 1005, 957, 922, 760, 687, 627, 600, 575. ^{1}H NMR (500 MHz, DMSO-d_6) δ 7.37–7.30 (m, 2H), 7.19 (td, J = 7.6, 1.2 Hz, 1H), 7.16 (s, 2H), 7.04 (dd, J = 8.2, 1.2 Hz, 1H), 4.79 (dd, J = 12.4, 5.2 Hz, 1H), 4.67 (dd, J = 12.4, 5.3 Hz, 1H), 4.32 (t, J = 5.2 Hz, 1H).

[9c-ii] 2-amino-7-bromo-4-(nitromethyl)-4*H*-1-benzopyran-3-carbonitrile [13]. White solid. IR (KBr) (ν_{max}, cm^{-1}): 3551, 3435, 3312, 3186, 3130, 3075, 3003, 2291, 1755, 1645, 1591, 1560, 1528, 1479, 1377, 1327, 1207, 1150, 1105, 1022, 957, 860, 727, 700.^{1}H NMR (500 MHz, Acetone-d_6) δ 7.64 (d, J = 2.3 Hz, 1H), 7.51 (dd, J = 8.7, 2.3 Hz, 1H), 7.04 (d, J = 8.7 Hz, 1H), 6.52 (s, 2H), 4.92 (dd, J = 12.7, 5.0 Hz, 1H), 4.78 (dd, J = 12.7, 5.0 Hz, 1H), 4.42 (t, J = 5.0 Hz, 1H).

[9c-iii] Methyl 2-amino-4-(nitromethyl)-4*H*-1-benzopyran-3-carboxylate [13]. White solid. IR (KBr) (ν_{max}, cm^{-1}): 3466, 3385, 3335, 3285, 3024, 2953, 2911, 1674, 1605, 1537, 1485, 1441, 1383, 1300, 1223, 1206, 1119, 1092, 1051, 1005, 854, 779, 758, 627. ^{1}H NMR (500 MHz, Chloroform-*d*) δ 7.32–7.28 (m, 1H), 7.20 (dd, J = 7.6, 1.8 Hz, 1H), 7.14 (td, J = 7.6, 1.2 Hz, 1H), 7.05 (dd, J = 8.2, 1.2 Hz, 1H), 6.46 (s, 2H), 4.66 (dd, J = 8.1, 4.4 Hz, 1H), 4.56 (dd, J = 11.4, 4.4 Hz, 1H), 4.41 (dd, J = 11.4, 8.1 Hz, 1H), 3.81 (s, 3H).

[9c-iv] Methyl 2-amino-6-bromo-4-(nitromethyl)-4*H*-1-benzopyran-3-carboxylate [NOVEL]. White solid. M.P. = 149 °C. IR (KBr) (ν_{max}, cm^{-1}): 3458, 3310, 3053, 2988, 2949, 1684, 1616, 1541, 1522, 1477, 1435, 1315, 1288, 1231, 1182, 1124, 1094, 1043, 1015, 876, 822, 783, 638, 608. ^{1}H NMR (500 MHz, Chloroform-*d*) δ 7.41 (dd, J = 8.7, 2.3 Hz, 1H), 7.35 (dd, J = 2.3, 0.6 Hz, 1H), 6.93 (d, J = 8.7 Hz, 1H), 6.50 (s, 2H), 4.60 (dd, J = 7.6, 4.2 Hz, 1H), 4.54 (dd, J = 11.8, 4.2 Hz, 1H), 4.45 (dd, J = 11.8, 7.6 Hz, 1H), 3.81 (s, 3H). ES(+) m/z = 344.98, 343.28, 299.11, 297.98, 284.87, 251.98.

[9c-v] Methyl 2-amino-6-chloro-4-(nitromethyl)-4*H*-1-benzopyran-3-carboxylate [NOVEL]. White solid. M.P. = 140 °C. IR (KBr) (ν_{max}, cm^{-1}): 3468, 3312, 3057, 3022, 2990, 2949, 1682, 1618, 1537, 1479, 1319, 1287, 1231, 1184, 1121, 1088, 1043, 1016, 829, 775, 648, 613. ^{1}H NMR (500 MHz, Chloroform-*d*) δ 7.26 (dd, J = 8.7, 2.5 Hz, 1H), 7.20 (d, J = 2.5 Hz, 1H), 6.99 (d, J = 8.7 Hz, 1H), 6.46 (s, 2H), 4.60 (dd, J = 7.7, 4.2 Hz, 1H), 4.54 (dd, J = 11.7, 4.2 Hz, 1H), 4.45 (dd, J = 11.7, 7.7 Hz, 1H), 3.81 (s, 3H). ^{13}C NMR (126 MHz, Chloroform-*d*) δ 168.45, 161.85, 148.51, 130.02, 129.02, 128.00, 123.46, 117.69, 80.69, 72.30, 51.32, 34.11. ES(+) m/z = 301.13, 299.05, 254.13, 252.15, 239.89, 208.07.

[9d-i] 2-amino-4-(2-hydroxynaphthalen-1-yl)-4*H*-1-benzopyran-3-carbonitrile [16]. White solid. M.P. 214 °C. IR (KBr) (ν_{max}, cm^{-1}): 3480, 3466, 3354, 3063, 2193, 1659, 1589, 1456, 1408, 1273, 1233, 1092, 1080, 1038, 847, 808, 752, 737, 716. ^{1}H NMR (500 MHz, DMSO-d_6) δ 9.81 (s, 1H), 7.96–7.87 (m, 3H), 7.48–7.39 (m, 2H), 7.30 (d, J = 8.9 Hz, 1H), 6.95 (ddd, J = 8.7, 7.2, 1.7 Hz, 1H), 6.87–6.78 (m, 4H), 6.63 (td, J = 7.5, 1.3 Hz, 1H), 5.58 (s, 1H).

[9e-i] 2-amino-4-(5-hydroxy-3-methyl-1*H*-pyrazol-4-yl)-4*H*-1-benzopyran-3-carbonitrile [48]. Yellow solid. M.P. 218 °C. IR (KBr) (ν_{max}, cm^{-1}): 3445, 3418, 3350, 3271, 3067, 2187, 1661, 1614, 1537, 1489, 1404, 1267, 1256, 1229, 1182, 1152, 1057, 868, 779. 768, 752, 700, 652. ^{1}H NMR (500 MHz, DMSO-d_6) δ 11.12 (s, 1H), 9.42 (s, 1H), 7.19 (ddd, J = 8.5, 6.9, 2.0 Hz, 1H), 7.07–6.99 (m, 2H), 6.95 (dd, J = 8.5, 1.1 Hz, 1H), 6.68 (s, 2H), 4.63 (s, 1H), 1.97 (s, 3H).

[9f-i] 7-(4-hydroxy-2-oxo-2*H*-chromen-3-yl)chromeno[4,3-*b*]chromen-6(7*H*)-one [49]. White solid. M.P. 250 °C. IR (KBr) (ν_{max}, cm^{-1}): 3063, 2968, 1697, 1605, 1489, 1456, 1389, 1219, 1105, 1049, 976, 905, 868, 752. ^{1}H NMR (500 MHz, Acetone-d_6) δ 8.17 (dd, J = 7.9, 1.7 Hz, 1H), 8.08 (d, J = 7.7 Hz, 1H), 7.73 (dd. D, J = 8.5, 7.4, 1.6 Hz, 1H), 7.62 (ddd, J = 8.3, 7.3, 1.6 Hz, 1H), 7.52 (ddd, J = 8.1, 7.3, 1.1 Hz, 1H), 7.44–7.37 (m, 2H), 7.36–7.34 (m, 2H), 7.33–7.29 (m, 1H), 7.28–7.22 (m, 1H), 7.20–7.12 (m, 1H), 5.72 (d, J = 0.8 Hz, 1H).

[10a] 2,4-diamino-5-(phenylsulfanyl)-5*H*-[1]benzopyrano[2,3-*b*]pyridine-3-carbonitrile [20]. Off-white solid. M.P. = 220 °C. IR (KBr) (ν_{max}, cm^{-1}): 3443, 3348, 3227, 3231, 3073, 2207, 1636, 1603, 1566, 1477, 1456, 1404, 1335, 1260, 1231, 1192, 1123, 1069, 899, 779, 758, 741, 696. ^{1}H NMR (500 MHz, DMSO-d_6) δ 7.29 (ddt, J = 8.7, 7.2, 1.5 Hz, 1H), 7.22–7.17 (m, 2H), 7.14–7.09 (m, 3H), 6.93 (s, 2H), 6.83–6.77 (m,

3H), 6.48 (s, 2H), 5.77 (s, 1H). ES(+) *m/z* = 346.96, 345.88, 236.96, 179.09, 175.68, 111.09, 76.75.

[10b] 2,4-diamino-8-bromo-5-(phenylsulfanyl)-5*H*- [1]benzopyrano [2,3-*b*] pyridine-3-carbonitrile [20]. Off-white solid. M.P. = 215 °C. IR (KBr) (ν_{max}, cm^{-1}): 3466, 3414, 3366, 3235, 3130, 2207, 1626, 1585, 1562, 1479, 1416, 1398, 1335, 1258, 1236, 1192, 1169, 1130, 1067, 824, 752, 737, 694. ^{1}H NMR (500 MHz, Acetone-d_6) δ 7.44–7.37 (m, 2H), 7.37–7.33 (m, 1H), 7.19 (dd, *J* = 8.5, 7.0 Hz, 2H), 6.94 (dd, *J* = 8.1, 1.4 Hz, 2H), 6.83 (d, *J* = 8.5 Hz, 1H), 6.46 (s, 2H), 5.98 (s, 2H), 5.68 (s, 1H).

[10c] 2,4-diamino-8-nitro-5-(phenylsulfanyl)-5*H*- [1]benzopyrano [2,3-*b*] pyridine-3-carbonitrile [20]. Yellow solid. M.P. = 207 °C. IR (KBr) (ν_{max}, cm^{-1}): 3439, 3348, 3198, 2189, 1651, 1611, 1537, 1520, 1408, 1339. 1258, 1088, 1022, 903, 837, 745, 691. ^{1}H NMR (500 MHz, Acetone-d_6) δ 8.21 (dd, *J* = 9.0, 2.7 Hz, 1H), 8.10 (dd, *J* = 2.8, 1.0 Hz, 1H), 7.74–7.67 (m, 2H), 7.54–7.48 (m, 3H), 7.31 (d, *J* = 9.0 Hz, 1H), 6.52 (s, 2H), 5.99 (s, 2H), 5.22 (s, 1H).

[10d] 2,4-diamino-8-chloro-5-(phenylsulfanyl)-5*H*- [1]benzopyrano [2,3-*b*] pyridine-3-carbonitrile [50]. Yellow solid. M.P. = 181 °C. IR (KBr) (ν_{max}, cm^{-1}): 3455, 3418, 3354, 3240, 3196, 2185, 1651, 1609, 1545, 1520, 1404, 1346, 1258, 1088, 818, 745^{1}H NMR (500 MHz, DMSO-d_6) δ 7.35–7.30 (m, 1H), 7.27 (dd, *J* = 8.7, 2.6 Hz, 1H), 7.20–7.14 (m, 2H), 7.08 (d, *J* = 2.6 Hz, 1H), 6.97 (s, 2H), 6.89–6.81 (m, 3H), 6.54 (s, 2H), 5.73 (s, 1H).

[10e] 2,4-diamino-5- [(4-methylphenyl)sulfanyl] -5*H*- [1]benzopyrano [2,3-*b*] pyridine-3-carbonitrile [50]. Orange solid. M. P. = 223 °C. IR (KBr) (ν_{max}, cm^{-1}): 3458, 3346, 3229, 3024, 2916, 2199, 1622, 1601, 1585, 1564, 1474, 1400, 1258, 1217, 1331, 1069, 812, 779, 752, 677, 642. ^{1}H NMR (500 MHz, DMSO-d_6) δ 7.24–7.17 (m, 2H), 7.11 (td, *J* = 7.4, 1.2 Hz, 1H), 6.95–6.87 (m, 4H), 6.82 (dd, *J* = 8.2, 1.2 Hz, 1H), 6.65 (d, *J* = 7.8 Hz, 2H), 6.47 (s, 2H), 5.70 (s, 1H), 2.24 (s, 3H).

[10f] 2,4-diamino-5-(4-bromophenylsulfanyl)-5*H*- [1]benzopyrano [2,3-*b*] pyridine-3-carbonitrile [51]. Yellow solid. M.P. = 230 °C. IR (KBr) (ν_{max}, cm^{-1}): 3416, 3345, 3242, 3163, 3073, 2205, 1570, 1472, 1454, 1406, 1335, 1260, 1215, 1198, 1065, 1007, 822, 791, 779, 760, 727, 702, 640. ^{1}H NMR (500 MHz, Acetone-d_6) δ 7.37 (dd, *J* = 7.7, 1.7 Hz, 1H), 7.33 (d, *J* = 7.9 Hz, 2H), 7.28 (ddd, *J* = 8.2, 7.3, 1.7 Hz, 1H), 7.17 (ddd, *J* = 7.7, 7.3, 1.2 Hz, 1H), 6.87 (dd, *J* = 8.2, 1.2 Hz, 1H), 6.77 (d, *J* = 7.9 Hz, 2H), 6.45 (s, 2H), 5.96 (s, 2H), 5.74 (s, 1H).

[10g] 2,4-diamino-7-nitro-5-(4-bromophenylsulfanyl)-5*H*- [1] benzopyrano [2,3-*b*] pyridine-3-carbonitrile [NOVEL]. Yellow solid. M.P. > 250 °C. IR (KBr) (ν_{max}, cm^{-1}): 3477, 3370, 3306, 3208, 2205, 1655, 1545, 1516, 1472, 1410, 1342, 1256, 1084, 1007, 837, 812, 746. ^{1}H NMR (500 MHz, Acetone-d_6) δ 8.23 (dd, *J* = 9.0, 2.7 Hz, 1H), 8.08 (dd, *J* = 2.7, 0.9 Hz, 1H), 7.68 (d, *J* = 8.6 Hz, 2H), 7.62 (d, *J* = 8.6 Hz, 2H), 7.31 (d, *J* = 9.0 Hz, 1H), 6.53 (s, 2H), 6.14 (s, 2H), 5.21 (s, 1H). 13C NMR (126 MHz, DMSO-d_6) δ 160.13, 153.62, 153.50, 144.24, 133.83, 132.93, 130.87, 124.86, 124.78, 123.35, 122.33, 119.93, 118.87, 118.22, 85.65, 54.29, 36.90. ES(+) *m/z* = 472.3, 390.15, 284.18, 256.84, 199.00.

[10h] 2,4-diamino-7-nitro-5-(4-methylphenylsulfanyl)-5*H*- [1] benzopyrano [2,3-*b*] pyridine-3-carbonitrile [51]. Yellow solid. M.P. = 218 °C. IR (KBr) (ν_{max}, cm^{-1}): 3418, 3354, 3240, 3196, 2185, 1651, 1609, 1545, 1520, 1346, 1258, 1088, 818. ^{1}H NMR (500 MHz, Acetone-d_6) δ 8.21 (dd, *J* = 9.0, 2.8 Hz, 1H), 8.08 (dd, *J* = 2.8, 0.9 Hz, 1H), 7.60 (d, *J* = 8.2 Hz, 2H), 7.35 (d, *J* = 8.3 Hz, 2H), 7.31 (d, *J* = 9.0 Hz, 1H), 6.50 (s, 2H), 5.88 (s, 2H), 5.20 (s, 1H), 2.41 (s, 3H).

[12a] 2- [4-(morpholin-4-yl)-5*H*- [1]benzopyrano [2,3-*d*] pyrimidin-2-yl] phenol [22]. Yellow solid. M.P. = 197 °C. IR (KBr) (ν_{max}, cm^{-1}): 3414, 3248, 3044, 2957, 2860, 1603, 1584, 1491, 1437, 1389, 1310, 1283, 1265, 1250, 1113, 1020, 953, 868, 835, 760. ^{1}H NMR (500 MHz, Chloroform-*d*) δ 13.13 (s, 1H), 8.44 (dd, *J* = 7.9, 1.8 Hz, 1H), 7.39 (ddd, *J* = 8.6, 7.1, 1.8 Hz, 1H), 7.31–7.28 (m, 1H), 7.23 (m, 2H), 7.15 (td, *J* = 7.3, 1.3 Hz, 1H), 7.01 (dd, *J* = 8.6, 1.2 Hz, 1H), 6.95 (ddd, *J* = 7.9, 7.1, 1.2 Hz, 1H), 3.97 (s, 2H), 3.94 (t, *J* = 4.9 Hz, 4H), 3.54 (t, *J* = 4.9 Hz, 4H). ^{13}C NMR (126 MHz, Chloroform-*d*) δ 164.78, 164.52–163.95 (m), 162.09, 160.39, 150.39, 133.00, 129.21, 128.58, 128.35, 124.56, 119.07, 118.90, 118.44, 117.64, 117.11, 97.73, 66.69, 48.67, 25.56. ES(+) *m/z* = 365.24, 364.10, 361.76, 343.10, 321.09, 292.18, 275.17, 170.93.

[12b] 2- [4-(piperidin-1-yl)-5*H*- [1]benzopyrano [2,3-*d*] pyrimidin-2-yl] phenol [22]. Yellow solid. M.P. = 168 °C. IR (KBr) (ν_{max}, cm^{-1}): 3451, 3046, 2940, 2855, 2835, 1603, 1584, 1454, 1368, 1310, 1258, 1242, 1190, 1113, 1007, 949, 837, 766. ^{1}H NMR (500 MHz, Chloroform-*d*) δ 13.43 (s, 1H), 8.43 (dd, *J* = 8.0, 1.8 Hz, 1H), 7.35 (ddd, *J* = 8.2, 7.2, 1.8 Hz, 1H), 7.25–7.23 (m, 1H), 7.23–7.18 (m, 2H), 7.11 (td, *J* = 7.4, 1.4 Hz, 1H), 6.98 (dd, *J* = 8.2, 1.2 Hz, 1H), 6.92 (ddd, *J* = 8.0, 7.2, 1.2 Hz, 1H), 3.93 (s, 2H), 3.44 (t, *J* = 5.2 Hz, 4H), 1.83–1.68 (m, 6H).

[12c] 2- [4-(pyrrolidin-1-yl)-5*H*- [1]benzopyrano [2,3-*d*] pyrimidin-2-yl] phenol [28]. Orange-brown solid. M.P. = 189 °C. IR (KBr) (ν_{max}, cm^{-1}): 3449, 3057, 2970, 2874, 1605, 1547, 1454, 1396, 1344, 1263, 1238, 1200, 1101, 962, 841, 754. ^{1}H NMR (500 MHz, Chloroform-*d*) δ 8.31 (dd, *J* = 8.0, 1.8 Hz, 1H), 7.26 (ddd, *J* = 8.2, 7.1, 1.8 Hz, 1H), 7.15 (td, *J* = 7.7, 7.1, 1.7 Hz, 1H), 7.06 (dd, *J* = 7.8, 1.7 Hz, 2H), 7.00 (td, *J* = 7.4, 1.3 Hz, 1H), 6.90 (dd, *J* = 8.2, 1.2 Hz, 1H), 6.82 (ddd, *J* = 8.0, 7.1, 1.2 Hz, 1H), 4.16 (s, 2H), 3.82–3.70 (m, 4H), 2.02–1.75 (m, 4H).

[12d] 2- [4-(dibutylamino)-5*H*- [1]benzopyrano [2,3-*d*] pyrimidin-2-yl] phenol [NOVEL]. White solid. M.P. = 115 °C. IR (KBr) (ν_{max}, cm^{-1}): 3449, 3051, 2961, 2934, 2874, 1605, 1584, 1535, 1493, 1443, 1377, 1260, 1240, 1111, 1072, 962, 839, 748. ^{1}H NMR (500 MHz, Chloroform-*d*) δ 8.42 (dd, *J* = 8.0, 1.8 Hz, 1H), 7.38 (ddd, *J* = 8.1, 7.1, 1.8 Hz, 1H), 7.30–7.25 (m, 1H), 7.25–7.21 (m, 2H), 7.13 (td, *J* = 7.3, 1.2 Hz, 1H), 7.04 (d, *J* = 8.0 Hz, 1H), 6.94 (ddd, *J* = 8.1, 7.1, 1.2 Hz, 1H), 4.02 (s, 2H), 3.59–3.48 (t, *J* = 7.7 Hz, 4H), 1.74–1.64 (m, 4H), 1.41 (h, *J* = 7.4 Hz, 4H), 0.99 (t, *J* = 7.4 Hz, 6H). ES(+) *m/z* = 405.15, 347.25, 304.21.

[12e] 2- [4-(diethylamino)-5*H*- [1]benzopyrano [2,3-*d*] pyrimidin-2-yl] phenol [30]. Orange solid. M.P. = 143 °C. IR (KBr) (ν_{max}, cm^{-1}): 3449, 2984, 2936, 1603, 1587, 1580, 1560, 1493, 1450, 1396, 1327, 1271, 1254, 1192, 1065, 841, 762. ^{1}H NMR (500 MHz, Chloroform-*d*) δ 8.42 (dd, *J* = 8.0, 1.7 Hz, 1H), 7.38 (ddd, *J* = 8.2, 7.1, 1.8 Hz, 1H), 7.28–7.25 (m, 1H), 7.21 (m, 2H), 7.13 (td, *J* = 7.4, 1.3 Hz, 1H), 7.03 (dd, *J* = 8.2, 1.2 Hz, 1H), 6.94 (ddd, *J* = 8.0, 7.1, 1.2 Hz, 1H), 4.05 (s, 2H), 3.61 (q, *J* = 7.1 Hz, 4H), 1.35 (t, *J* = 7.1 Hz, 6H).

[12f] 4-bromo-2- [7-bromo-4-(morpholin-4-yl)-5*H*- [1]benzopyrano [2,3-*d*] pyrimidin-2-yl] phenol [22]. Yellow solid. M.P. = 195 °C. IR (KBr) (ν_{max}, cm^{-1}): 3408, 2972, 2895, 2853, 1597, 1543, 1483, 1433, 1369, 1277, 1248, 1182, 1121, 1028, 959, 872, 827, 733, 631. ^{1}H NMR (500 MHz, Chloroform-*d*) δ 13.04 (s, 1H), 8.50 (d, *J* = 2.5 Hz, 1H), 7.45 (dd, *J* = 8.8, 2.5 Hz, 1H), 7.40 (m, 2H), 7.10 (d, *J* = 9.3 Hz, 1H), 6.89 (d, *J* = 8.8 Hz, 1H), 3.96–3.91 (m, 6H), 3.52 (t, *J* = 4.7 Hz, 4H).

[12g] 4-bromo-2- [7-bromo-4-(piperidin-1-yl)-5*H*- [1]benzopyrano [2,3-*d*] pyrimidin-2-yl] phenol [22]. Yellow solid. M.P. = 222 °C. IR (KBr) (ν_{max}, cm^{-1}): 3445, 3069, 2940, 2851, 1599, 1543, 1487, 1435, 1369, 1256, 1184, 1256, 1184, 1101, 1009, 822, 746. ^{1}H NMR (500 MHz, Chloroform-d) δ 8.44 (d, *J* = 2.6 Hz, 1H), 7.34 (dd, *J* = 8.7, 2.6 Hz, 1H), 7.32–7.27 (m, 2H), 7.01 (d, *J* = 8.3 Hz, 1H), 6.79 (d, *J* = 8.7 Hz, 1H), 3.84 (s, 2H), 3.37 (t, *J* = 5.1 Hz, 4H), 1.74–1.64 (m, 6H).

[12h] 4-chloro-2- [7-chloro-4-(morphin-4-yl)-5*H*- [1]benzopyrano [2,3-*d*] pyrimidin-2-yl] phenol [22]. Yellow solid. MP > 250 °C. IR (KBr) (ν_{max}, cm^{-1}): 3335, 3071, 2968, 2893, 2857, 1601, 1560, 1547, 1483, 1429, 1371, 1364, 1261, 1248, 1184, 1121, 1022, 964, 874, 822, 748, 700, 654. 1H NMR (500 MHz, Chloroform-d) δ 8.37 (d, *J* = 2.7 Hz, 1H), 7.35–7.30 (m, 1H), 7.28–7.24 (m, 2H), 7.16 (dt, *J* = 9.0, 1.3 Hz, 1H), 6.95 (d, *J* = 8.8 Hz, 1H), 3.99–3.90 (m, 6H), 3.52 (t, *J* = 4.8 Hz, 4H).

[12i] 4-chloro-2- [7-chloro-4-(piperidin-1-yl)-5*H*- [1]benzopyrano [2,3-*d*] pyrimidin-2-yl] phenol [22]. Yellow solid. M.P. >250 °C. IR (KBr) (ν_{max}, cm^{-1}): 3327, 3071, 2968, 2893, 2857, 1601, 1547, 1483, 1429, 1364, 1248, 1184, 1121, 1022, 964, 874, 822, 748, 700, 654. ^{1}H NMR (500 MHz, Chloroform-*d*) δ 8.40 (d, *J* = 2.7 Hz, 1H), 7.31 (dd, *J* = 8.7, 2.7 Hz, 1H), 7.27–7.23 (m, 2H), 7.18–7.13 (m, 1H), 6.95 (d, *J* = 8.7

Hz, 1H), 3.94 (s, 2H), 3.48 (t, J = 5.1 Hz, 4H), 1.87–1.70 (m, 6H).

3. Results and discussion

3.1. Catalyst basicity determination and characterization

Following catalyst screening, the chosen catalyst for all three reaction-types was piperazine supported on Amberlyst® 15 beads (which were subsequently crushed and ground). Different preparation methods were tried in order to synthesize the novel catalyst (as per experimental section). The below are the loadings (by mass difference) obtained for each piperazine catalyst along with basicity (determined by back-titration):

- **Pip-A15-A** – loading by mass = 2.72 mmol/g; basicity as per titration = 1.44 mmol/g
- **Pip-A15-B** – loading by mass = 2.10 mmol/g; basicity as per titration = 1.39 mmol/g
- **Pip-A15-C** – loading by mass = 2.10 mmol/g; basicity as per titration = 1.38 mmol/g
- **Pip-A15-D** – loading by mass = 2.00 mmol/g; basicity as per titration = 1.39 mmol/g
- **Pip-A15-E –** loading by mass = 2.10 mmol/g; basicity as per titration = 1.40 mmol/g
- **Pip-A15-F –** loading by mass = 1.20 mmol/g; basicity as per titration = 1.0 mmol/g
- **Pip-A15-G** – loading by mass = 0.71 mmol/g; basicity as per titration - negligible

The reasons behind the different loadings can be explained as follows: when the catalyst was prepared at room temperature (first method), it was highly likely that a fraction of piperazine entered and got trapped within the Amberlyst® 15 polymeric matrix but remained unreacted. As a result, the loading by mass was significantly high (2.72 mmol/g). Washing repeatedly with ethanol did not cause any catalyst mass changes which signifies that physisorption was significantly strong. On heating the prepared catalyst to 110–120 °C in a round bottomed flask under vacuum, the loading decreased to 2.1 mmol/g (Pip-A15-B) possibly because unreacted piperazine sublimed. In the methods involving reflux (second method), if piperazine got trapped within the Amberlyst® 15 matrix, it was highly likely that with time, the kinetically energetic solvent molecules dislodged the unreacted piperazine to transfer it back to solution resulting in a lower loading of 2.1 mmol/g (**Pip-A15-C, D, E**). Lastly, when the polymeric beads were crushed before carrying out the stirring with piperazine (**Pip-A15-F**), the loading was lower because piperazine had less polymeric matrix volume in which it could reside and react with the sulfonic acid groups. In other terms, the A15 pores were no longer available to act as microreactors.

The acid content of unloaded dry Amberlyst® 15 was found to be equal to 3.0 mmol/g. This makes sense as per following explanation. When the Pip-A15 loading was equal to 2.1 mmol/g (in Pip-A15-B, C, D, E), since the basicity (as per titration) was equal to 1.40 mmol/g, that leaves (2.1–1.40) 0.7 mmol/g of piperazine bonded to two equivalents of sulfonic acid groups. Multiplying the latter value by 2 and adding it to the value of 1.40 mmol/g should give the total number of sulfonic acid being involved in bonding (1.40 + 1.40 = 2.8 mmol/g) which value is fairly similar to the total acid content of dry Amberlyst® 15.

Bearing all of the above in mind, the two possible structures for Pip-A15 are those portrayed in Fig. 2 with structure **A** being responsible for donning basicity to the catalyst and structure **B** making up the remaining amount of loaded piperazine.

Amongst the IR spectra displayed in Table 1, the first two entries highlight the differences between the functionalities of Amberlyst® 15 (the support) and the catalyst (Pip-A15-A). Firstly, the addition of piperazine to Amberlyst® 15 caused a slight change in the IR spectrum as seen by introduction of bands at 3248 and 3211 cm^{-1} caused by the NH stretching and the NH bending overtone of the free NH (1st harmonic is at 1628 cm^{-1}) group respectively. At 2855 cm^{-1} the band present could be due to the N–H stretch of the piperazinium end. Bands at 1464, 1441, 1410 are caused by the aromatic C–H stretches of the phenyl rings in A15 [52]. The band at 1180 cm^{-1} has been attributed to the stretching vibration of the O═S═O group. Close by, the bands at 1126 and 1086 cm^{-1} are evidence of in-plane skeletal C–H vibrations of a disubstituted benzene ring. A minor band at 741 cm^{-1} is assignable to C–S–C symmetric stretching whereas those at 866, 833 and 673 cm^{-1} are caused by aromatic out-of-plane C–H vibrations [52]. The catalyst with a lower loading (Pip-A15-B) gave an identical spectrum.

Further to the above, the recovered catalysts after the recycling runs for the synthesis of the *4H*-chromene **9b-i,** the chromeno[2,3-*b*]pyridine **10a** and the chromeno[2,3-*d*]pyrimidine **12a** were also analysed. In fact, it is quite evident that the IR spectra were very similar to that of the fresh catalyst. For instance, the NH stretch and bending overtone band are both particularly clear and visible at 3285 and 3211 cm^{-1} for the catalyst collected after the synthesis of **12a.** However, in the spectra of the recycled catalysts following the synthesis of **9b-i** and **10a**, the latter characteristic bands appear less evident.

3.2. Optimisation runs

Initially, the model reaction (Table 2) between malononitrile (**1a**), salicylaldehyde (**2a**) and thiophenol (**3a**) was attempted under various heterogeneous catalysts out of which Pip-A15, DABCO-SiO_2 and DABCO-A15 appeared to give the best results, with Pip-A15-A (2.72 mmol/g loading) in particular giving the highest yield of compounds **9a-i** after

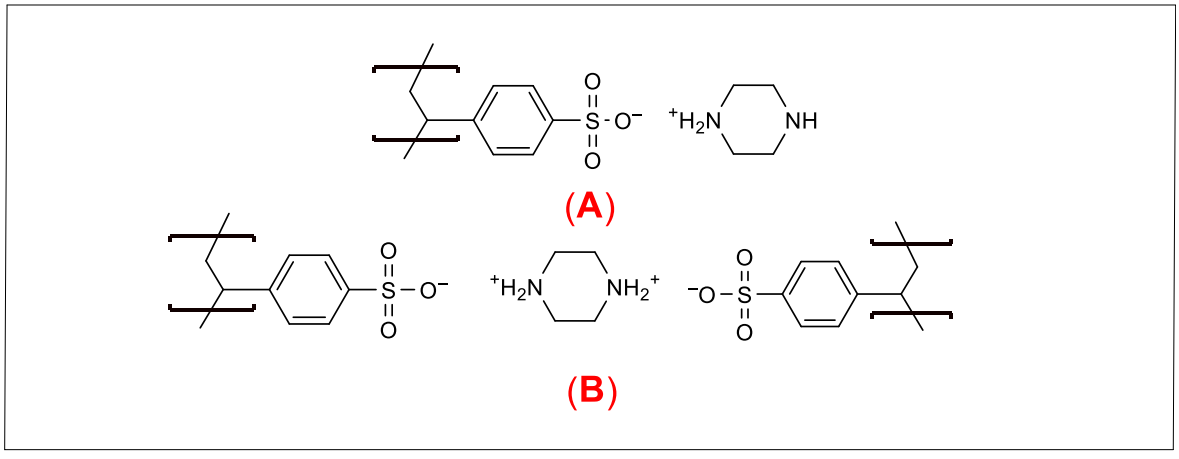

Fig. 2. Possible structures of Amberlyst®15-Piperazine.

Table 1
IR spectra of Amberlyst® 15 and Pip-A15 (% transmittance vs wavenumber (cm^{-1}).

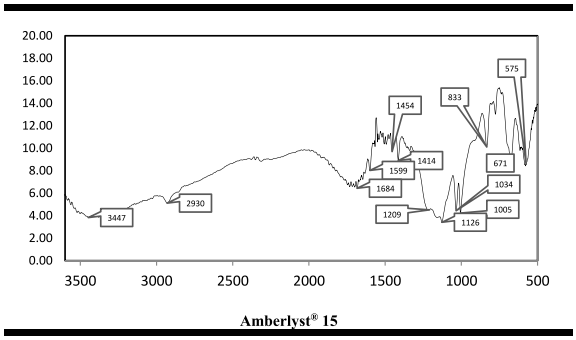

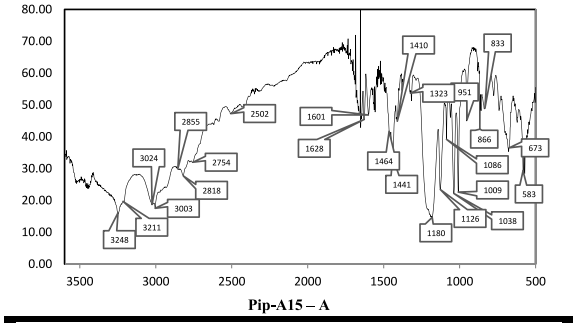

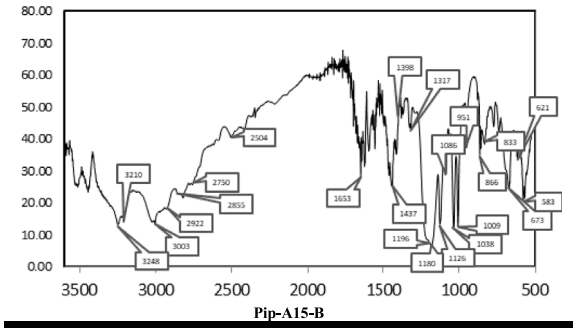

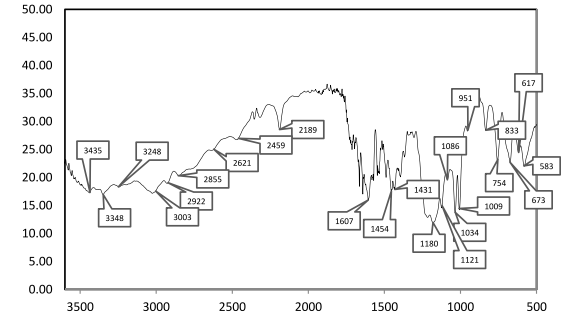

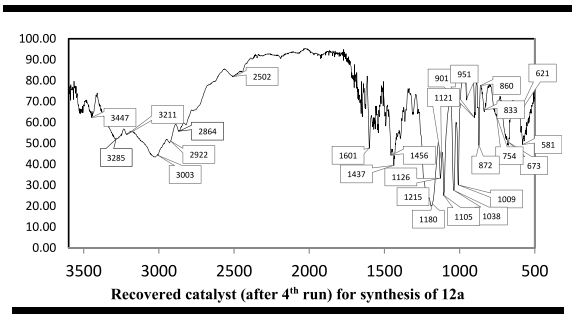

mixing at 50 °C for 8 h in ethanol solvent (82%, **entry 2**, Table 2). When the reaction was performed at a higher temperature, several side products were formed including the chromeno[2,3-*b*]pyridine (**entry 3,** Table 2). Alternatively, when conducted in neat conditions, the reaction stopped at the intermediate stage after solidification took place within 10 min (**entry 4,** Table 2). Interestingly, when the reaction was performed at room temperature another side product appeared to form which could not be isolated (^{1}H NMR of precipitated product gave a mixture of peaks). Decreasing the amount of catalyst proved detrimental because the yield dipped to 70% (**entry 6**). When the same ideal conditions (i.e. T = 50 °C, 10 mol% Pip-A15 - A (2.72 mmol/g) catalyst, ethanol solvent) were extended to 2-methylindole (corresponding products **9b-i)**, a good yield was obtained (**entry 13,** Table 2); which value was not mirrored by DABCO-SiO_2 (**entry 12,** Table 2).

In a series of further optimisation runs, differently prepared Pip-A15 catalyst batches were tested. Pip-A15 – B in the form of beads performed poorly even on increasing reaction time to 8 h (**entry 14,** Table 2). Crushing and pulverising the latter catalyst gave a higher yield of 57% (**entry 16,** Table 2) that increased further to 66% on increasing the catalytic equivalence to 15 mol% (**entry 17,** Table 2). Trialling again the catalyst in the form of beads but at a slightly higher temperature (**entry 15,** Table 2) did not even furnish any product. It was only when the molar loading was increased to 20 mol% that an excellent yield of 81% was once more attained (**entry 18,** Table 2), albeit at a longer reaction time. Using 10 mol% of catalyst Pip-A15 – E gave only a yield of 43% (**entry 19,** Table 2) whereas the even lower loaded catalyst Pip-A15 - F did not furnish any product at all (**entry 20,** Table 2) which was to be expected considering the negligible basicity. As will be discussed later on, since the reaction was conducted at only 50 °C, the use of Pip-A15-A did not result in piperazine leaching which means that it could be recycled successfully.

The trials involving nitromethane (corresponding products **9c-i**), generally provided poorer yields possibly due to the instability of the final product (**entries 21**–**24,** Table 2). Yet, Pip-A15-A once again surpassed other catalysts in terms of activity. Lastly, 2-naphthol (corresponding products **9d-i**), proved to be a very unreactive species with no particular catalyst (**entries 25**–**34,** Table 2) yielding the product except for DBU-SiO_2 and the chosen catalyst, Pip-A15-A. The former performed slightly better in light of the fact that DBU ($pK_b = 2$) is a much stronger base than piperazine. The reason behind the poor result is three-fold: 1) 2-naphthol is less likely to undergo electrophilic substitution than 2-methylindole keeping in mind that the hydroxyl group activates the ring in the former less than the nitrogen in the latter; 2) 2-naphthol is quite bulky and probably was sterically hindered from reacting with the Knoevenagel intermediate; 3) The reaction turned very dark even when performed under nitrogen which goes to show that decomposition was actively taking place.

Having established Pip-A15 as the ideal catalyst for 2-amino-4*H*-chromene (**9**) synthesis, the same catalyst was trialled, along with other catalysts, throughout the optimisation runs for the synthesis of chromeno [2,3-*b*]pyridines (**10**) as summarised in Table 3. As evidenced, Pip-A15 -A gave the best result when utilised at 10 mol% in ethanol solvent (Table 3**, entry 6**). In addition, subsequent trials showed that the choice of solvent had a massive impact on the reaction. In fact, on moving from ethanol to more polar mixtures/solvents such as methanol or 7:3 ethanol/water, the reaction mixture turned completely dark and viscous, and no product could be obtained after the DMF/water addition (Table 3**, entries 10**–**12**).

Regretfully, the reaction could not be monitored by GC because the product probably had a boiling point which was too high to allow for it to volatilize and get carried along in the GC column. Furthermore, reaction monitoring by TLC proved troublesome because the intermediate chromene spot never disappeared completely. As a result, the reaction had to be left ongoing for different amounts of time to try to establish when it had reached a state of equilibrium. In relation to this, when the reaction was left stirring, at the ideal conditions, for either 3 or 5 h instead of 4 h (Table 3**, entry 6**), the product yield was inferior in both cases.

Table 2
Catalyst screening and optimisation runs for the synthesis of 2-amino-4*H*-chromenes (**9**) from malononitrile (**1a**), salicylaldehyde (**2a**) and a nucleophilic species (**3**–**7**/**8**).

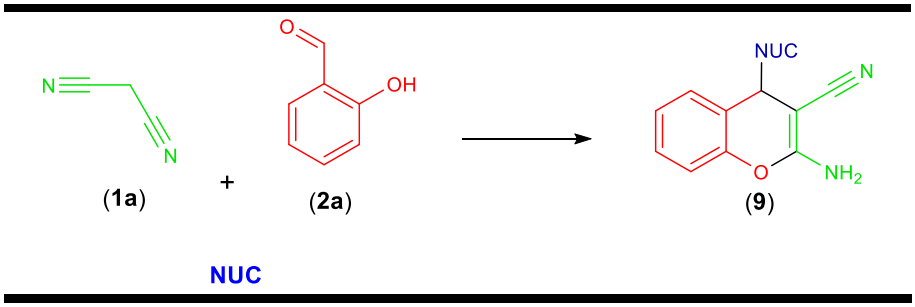

Entry[a]	Nucleophile	Catalyst (loading)	Amount of catalyst	Temperature [°C]/Time (hrs)	Yield (%) (Product code)
1[b]	Thiophenol (3a)	DABCO-SiO_2[c] (0.9 mmol/g)	10 mol%	50/8	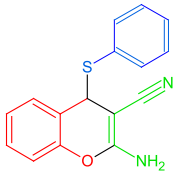 80% **(9a-i)** 82%
2[b]		Pip-A15-A (powder) (2.72 mmol/g)	10 mol%	50/8	
3[b]			10 mol%	80/2	Imp[d]
4[e]			10 mol%	50/0.16	Int.[f]
5[b]			10 mol%	RT/24	43%
6[b]			5 mol%	50/8	70%
7[b]		DABCO-A15 powder (2.86 mmol/g)	10 mol%	50/8	79%
8[b]		WSi-MKSF[g] (0.1 mmol/g)	0.4 mol%	50/8	N/A
9[b]		KF-Al_2O_3[h] (3.0 mmol/g)	10 mol%	50/8	60%
10[b]		Acidic Al_2O_3	0.25 g	50/8	N/A
11[b]		A15 (dry, beads)	0.25 g	50/8	N/A
12[i]	2-Me-Indole (4a)	DABCO-SiO_2 (0.9 mmol/g)	10 mol%	50/24	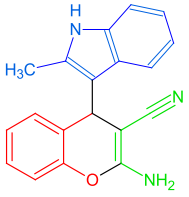 46% **(9b-i)** 82%
13[i]		Pip-A15-A (powder) (2.72 mmol/g)	10 mol%	50/5	
14		Pip-A15-B[j] (beads) 2.1 mmol/g	10 mol%	50/8	29%
15		Pip-A15-B[j] (beads) 2.1 mmol/g	10 mol%	60/8	Traces
16		Pip-A15-B[k]	10 mol%	50/5	57%
17		(powder)	15 mol%	50/10	66%
18		(2.1 mmol/g)	20 mol%	50/10	81%
19		Pip-A15-F (powder) 1.2 mmol/g	10 mol%	50/10	43%
20		Pip-A15-G (powder) (0.71 mmol/g)	10 mol%	50/10	Traces
21[b]	Nitromethane (5)	DABCO-SiO_2 (0.9 mmol/g)	10 mol%	50/3	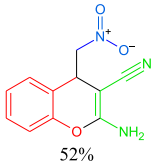 52% **(9c-i)** 61%
22[b]		Pip-A15-A (powder) (2.72 mmol/g)	10 mol%	50/3	

(*continued on next page*)

Table 2 (*continued*)

Entry[a]	Nucleophile	Catalyst (loading)	Amount of catalyst	Temperature [°C]/Time (hrs)	Yield (%) (Product code)
23[b]			10 mol%	60/4	N/A
24[b]			10 mol%	80/3	–
25	2-Naphthol (6)	WSi-MKSF (0.1 mmol/g)	0.4 mol%	RT/24	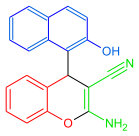 - (**9d-i**)
26		Acidic alumina	0.3 g	RT/24	N/A
27		CuI-A21[l] (1.34 mmol/g)	10 mol%	RT/24	N/A
28		CaO	0.2 g (140 mol%)	RT/48	N/A
29		KF-Al_2O_3 (3.0 mmol/g)	0.3 g (50 mol%)	RT/24	N/A
30		A26 (dry)[m]	0.5 g	60/48	N/A
31		DABCO-A15 (2.80 mmol/g)	10 mol%	50/14	N/A
32[b,n]		DBU-SiO_2[o] (0.6 mmol/g)	10 mol%	50/3	38%
33[b,n]		Pip-A15 – A (powder) (2.72 mmol/g)	10 mol%	55/14	25%
34		DABCO-SiO_2 (0.9 mmol/g)	10 mol%	50/3	N/A

[a] Reactions were performed on a 2.5 mmol scale in the presence of 4 mL ethanol solvent using a 1 (salicylaldehyde): 1 (malononitrile): 1 (nucleophilic reagent) molar ratio.
[b] Yield of pure purified product confirmed by ^{1}H NMR, IR. Purification was performed by column chromatography.
[c] Silica-bonded CPTMS DABCO (method in experimental section).
[d] An impure product mixture was obtained probably containing the chromeno[2,3-*b*]pyridine.
[e] Reaction performed in neat conditions until solidification took place (approx. 10 min) and stirring couldn't continue;
[f] Intermediate only formed.
[g] Silicotungstic acid supported on Montmorillonite KSF (method in experimental section).
[h] Potassium fluoride supported on alumina.
[i] Yield of pure purified product confirmed by ^{1}H NMR and IR. Purification was performed by recrystallization from 99% ethanol.
[j] Reaction was performed using Pip-A15 in the form of beads rather than as powder.
[k] Reaction was performed using Pip-A15 with a lower piperazine loading (2.1 mmol/g).
[l] Copper(I) iodide supported on Amberlyst® A21.
[m] Dry Amberlyst® A26 beads.
[n] Reaction performed under nitrogen.
[o] Silica-bonded CPTMS DBU.

When reaction was performed in a stepwise fashion at 50 °C by first mixing 1 equivalent of each reactant for 8 h to form the 4*H*-chromene and then adding another equivalent of malononitrile and mixing for a further 4 h, a lower yield was attained (Table 3**, entry 7**). Moreover, the decrease in temperature to 70 °C proved detrimental as well (Table 3**, entry 8**, 46% yield). Interestingly, the strongly basic DBU-SiO_2 and KF-Zeolite provided poor yields as did ZrO_2–NH_2 and Cell-NH_2 (Table 3**, entries 14**–**19**). Chit-NH_2 fared better (**entry 20,** 64% yield) but still performed worse than Pip-A15.

Positively, the synthesis of benzopyrano[2,3-*d*]pyrimidines (**12**) from malononitrile (**1a**), salicylaldehyde (**2a**) and morpholine (**11a**) was also successfully conducted using Pip-A15-A which gave the highest yield in amongst a wide array of tried catalysts (Table 4). Initially, most of the catalysts were utilised at 80 °C and Pip-A15-A (10 mol%) gave the best result at this condition (Table 4**, entry 12**). Subsequently, condition optimisation was conducted by changing the solvent, temperature, reactants' ratios and catalyst amount to get the highest yield of 70% (Table 4**, entry 29**).

When Pip-A15-B was tried (Table 4**, entry 32**) a lower yield was obtained even after leaving the reaction to take place for slightly longer (6 h). This was to be expected considering the absence of unreacted piperazine within the polymer matrix.

3.3. *Expanding the substrate scope*

For the first group of products (the 4*H*-chromenes), (**9**) salicylaldehyde (**2a**) was reacted with malononitrile (**1a**) or methyl cyanoacetate (**1b**) and a different range of nucleophilic substrates (**3**) (indoles, thiols, nitromethane and hydrazine/ethyl acetoacetate, 2-naphthol) to give the products usually in reasonable yields (Table 5, 15–82%, 17 examples). Overall, malononitrile provided the best results in terms of its role as an activated-methylene-containing compound. In addition, generally, the best results were obtained when using unsubstituted salicylaldehyde. In fact, both when electron-poor aldehydes (halogen or nitro substituted) and electron-rich (hydroxy substituted) were used, the yields were generally lower. An electron-poor aldehyde should be able to react faster with the methylene active compound to form the Knoevenagel intermediate. Subsequently, the intermediate would be more prone to nucleophilic attack; something which appears to counter the general yield trends. Moreover, the intermediate could itself react with for example another equivalent of the methylene-active compound to furnish a side product (Fig. 3 **- A**). Not only, but the latter can even react further with another equivalent of malononitrile to form the chromeno[2,3-*b*]pyridine (Fig. 3 **– B**) (this was isolated, ^{1}H NMR in Supplementary information).

As underscored previously, nucleophilic substances varied in their ability to react. For instance, 2-methylindole performed better than indole (Table 5, **entry 6** vs **7**) possibly because the steric hindrance and reactivity site-blocking created by the methyl group at C2 in 2-methylindole, hindered the possibility of side reactions. In addendum, thiols may be slightly better nucleophiles than indoles as can be understood from comparison of **entries 2** and **8** (Table 5) in their separate reaction with 5-bromosalicylaldehyde and malononitrile. On the other hand,

Table 3
Catalyst screening and optimisation runs for the synthesis of the benzopyrano[2,3-*b*]pyridine (**10a**) derived from malononitrile (**1a**) salicylaldehyde (**2a**) and thiophenol (**3a**).

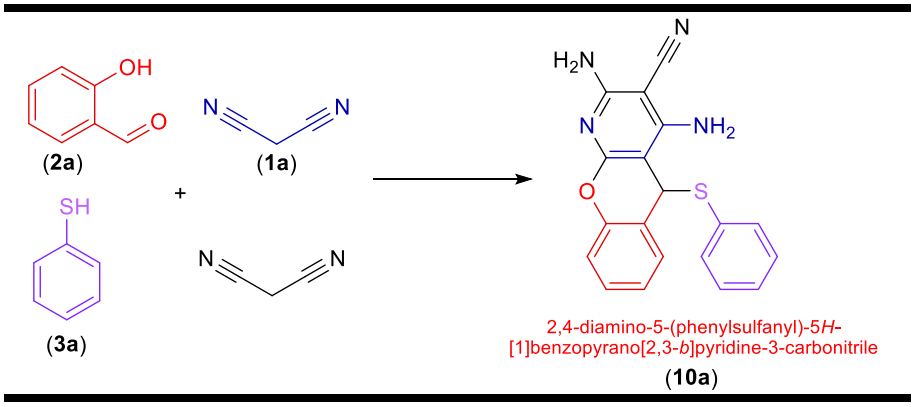

Entry[a]	Catalyst (loading)	Amount of catalyst	Solvent	Temperature [°C]/Time (hrs)	Yield (%)[b]
1	DABCO-SiO_2[c]	10 mol%	EtOH	70/4	44%
2	(1.00 mmol/g)	10 mol%	EtOH	RT/20	N/A
3		10 mol%	EtOH	80/2	48%
4		10 mol%	EtOH	80/4	61%
5	DABCO-A15 (powder) (2.80 mmol/g)	20 mol%	EtOH	80/4	63%
6	Pip-A15-A (powder) (2.72 mmol/g)[d]	10 mol%	EtOH	80/4	74%
				80/3	65%
				80/5	62%
7		10 mol%	EtOH	50/8 + 4	61%
8		10 mol%	EtOH	70/4	46%
9		10 mol%	EtOH	50/10	67%
10		10 mol%	EtOH–H_2O (7 : 3)	80/5	N/A
11		10 mol%	EtOH–H_2O (8 : 2)	80/4	N/A
12		10 mol%	MeOH	80/4	N/A
13	PW-Al_2O_3[e] (0.1 mmol/g)	1.5 mol%	EtOH	70/30	29%
14	DBU-SiO_2[f]	10 mol%	EtOH	RT/24	N/A
15	(0.6 mmol/g)	10 mol%	EtOH	80/4	36%
16	KF-Zeolite[g]	20 mol%	EtOH	RT/24	N/A
17	(3.4 mmol/g)	20 mol%	EtOH	80/4	54%
18	ZrO_2–NH_2[h] (0.6 mmol/g)	10 mol%	EtOH	80/4	43%
19	Cell-NH_2[i] (0.9 mmol/g)	10 mol%	EtOH	80/4	45%
20	Chit-NH_2[j] (0.9 mmol/g)	10 mol%	EtOH	80/4	64%

[a] Reactions performed on a 2.5 mmol scale using a molar ratio of 1 (salicylaldehyde): 1 (thiophenol): 2 (malononitrile) in ethanol solvent in one-pot.
[b] Yield of pure isolated product confirmed by ^{1}H NMR. Product was purified by dissolving in enough DMF and then adding deionised water to precipitate out the product.
[c] Silica-bonded CPTMS-DABCO (method in experimental section).
[d] Catalyst was crushed with hammer and ground using pestle and mortar.
[e] 40% w/w phosphotungstic acid supported on alumina (method in experimental section).
[f] Silica-bonded CPTMS-DBU (method in experimental section).
[g] KF supported on clinoptilolite zeolite (method in experimental section).
[h] APTES-treated zirconia (h) or cellulose.
[i] or chitosan.
[j] (method in experimental section).

nitromethane (**5**) and 2-naphthol (**6**) both were inferior as nucleophiles in reactions also involving malononitrile (Table 5**, entries 11, 12, 13**). Interestingly, the use of methyl acetoacetate provided better results when nitromethane was involved whereas 2-methylindole barely reacted (Table 5**, entries 16–18**). In a further development, an attempt at converting the three-component reaction to a four-component one proved successful when the nucleophilic substance was formed by an *in situ* reaction between the added hydrazine (**7**) and ethyl acetoacetate (**8**) (Table 5**, entry 14**).

Turning to the substrate scope of chromeno[2,3-*b*]pyridines (**10a – h**), although the general yields were lower, the trends observed earlier reperpetrated themselves. For instance, halogen- and nitro-substituted (**entries 2–4,** Table 6) salicylaldehydes provided poorer yields than salicylaldehyde itself.

Lastly, in the synthesis of chromeno[2,3-*d*]pyrimidines (**12**) (Table 7), the use of halogen and nitro substituted salicylaldehydes (Table 7**, entries 5–8**) once again manifested detrimental to the yield (compared to that obtained using salicylaldehyde). More so, nitro substituted salicylaldehyde (Table 7**,** entries **9–10**) did not furnish any product at all.

Table 4
Catalyst screening and condition optimisation for the synthesis of the chromeno[2,3-*d*]pyrimidine (**12a**) derived from malononitrile (**1a**), salicylaldehyde (**2a**) and morpholine (**11a**).

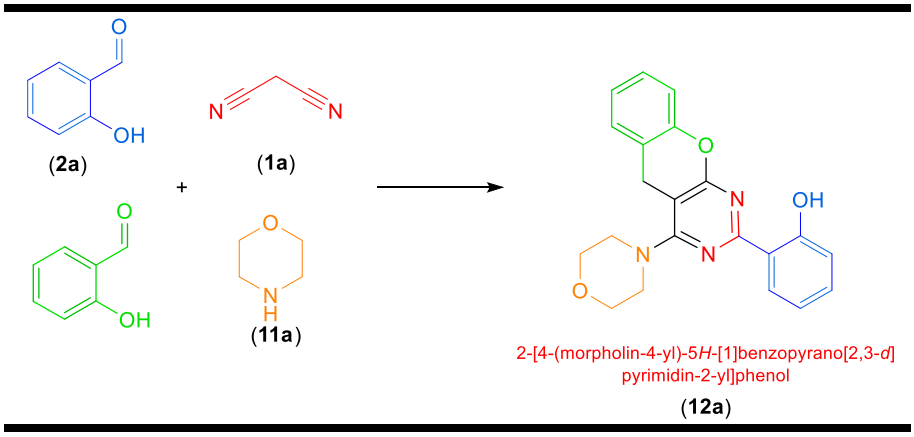

Entry[a]	Catalyst (loading)	Amount of catalyst	Solvent/Amount (mL)	Temperature [°C]/Time (hrs)	Reactant ratio	Yield (%)[b]
1	DABCO-A15 (powder)[c] (2.8 mmol/g)	10 mol%	EtOH/4	80/4	2 : 1: 1	40%
2	DABCO-SiO_2 (0.9 mmol/g)	10 mol%	EtOH/4	80/4	2 : 1: 1	25%
3	SiO_2-DABCO-SO_3H[d] (0.8 mmol/g)	10 mol%	EtOH/4	60/4	2 : 1: 1	33%
4	DBU-SiO_2	5 mol%	EtOH/4	80/4	2 : 1: 1	47%
5	(0.6 mmol/g)	10 mol%	EtOH/4	80/4	2 : 1: 1	38%
6	DBU-A15[e]	10 mol%	EtOH/4	80/12	2 : 1: 1	26%
7	(2.2 mmol/g)	10 mol%	EtOH/4	60/12	2 : 1: 1	39%
8		20 mol%	EtOH/4	80/4	2 : 1: 1	27%
9	Pip-SiO_2[f]	10 mol%	EtOH/4	RT/24	2 : 1: 1	34%
10	(1.8 mmol/g)	20 mol%	EtOH/4	RT/24	2 : 1: 1	42%
11		10 mol%	EtOH/4	80/24	2 : 1: 1	37%
12	Pip-A15-A (powder)	5 mol%	EtOH/4	80/8	2 : 1: 1	65%
13	(2.72 mmol/g)	10 mol%	EtOH/4	80/4	2 : 1: 1	60%
14		10 mol%	ETOH/4	60/8	2 : 1: 1	66%
				60/24		66%
15		10 mol%	EtOH/10	60/4	2 : 1: 1	50%
16		10 mol%	EtOH/4	80/8	2 : 1: 1	46%
17		12 mol%	EtOH/4	70/4	2 : 1: 1	56%
18		15 mol%	EtOH/4	60/4	2 : 1: 1	63%
19		25 mol%	EtOH/4	60/24	2 : 1: 1	63%
20		10 mol%	96% EtOH/4	70/4	2 : 1: 1	46%
21		10 mol%	7 : 3 EtOH/H_2O/4	60/4	2 : 1: 1	52%
22		5 mol%	MeOH/4	70/4	2 : 1: 1	60%
23		10 mol%	MeOH/4	RT/48	2 : 1: 1	50%
24		10 mol%	MeOH/4	50/36	2 : 1: 1	48%
25		10 mol%	MeOH/4	60/4	2 : 1: 1	64%
26		10 mol%	MeOH/4	60/4	2 : 1: 1.5	61%
27		10 mol%	MeOH/4	70/4	2 : 1: 1.5	53%
28		10 mol%	MeOH/4	70/8	2 : 1: 1	68%
29		10 mol%	MeOH/4	70/4	2 : 1: 1	70%
30		12 mol%	MeOH/4	70/8	2.2 : 1.1 : 1	55%
31		12 mol%	MeOH/4	70/4	2 : 1: 1	66%
32	Pip-A15-B (powder) 2.1 mmol/g	10 mol%	MeOH/4	70/6	2 : 1: 1	64%
33	EDA-A15 (powder)[g] (2.0 mmol/g)	10 mol%	EtOH/4	80/4	2 : 1: 1	57%
34	KF-Zeolite (3.4 mmol/g)	20 mol%	EtOH/4	80/4	2 : 1: 1	32%
35	$MeSO_3H$–Al_2O_3[h] (0.5 mmol/g)	10 mol%	EtOH/4	80/4	2 : 1: 1	46%
36	PW-Al_2O_3 (0.1 mmol/g)	1.2 mol%	EtOH/4	80/4	2 : 1: 1	43%
37	WSi–Al_2O_3[i] (0.1 mmol/g)	2.4 mol%	EtOH/4	80/4	2 : 1: 1	43%
38	WSi-A15[j] (0.1 mmol/g)	1.2 mol%	EtOH/4	80/6	2 : 1: 1	33%
39	SO_4^{2-}/ZrO_2[k] (2.08 mmol/g as SO_4^{2-})	30 mol%	EtOH/4	80/4	2 : 1: 1	42%

(*continued on next page*)

Table 4 (*continued*)

Entry[a]	Catalyst (loading)	Amount of catalyst	Solvent/Amount (mL)	Temperature [°C]/Time (hrs)	Reactant ratio	Yield (%)[b]
40	SO_4^{2-}/Al_2O_3[l]	16 mol%	EtOH/4	80/4	2 : 1: 1	44%
41	(2.08 mmol/g as SO_4^{2-})	20 mol%	EtOH/4	80/4	2 : 1: 1	48%
42	Amberlyst® A26 (dry)	16 mol%[c]	EtOH/4	80/4	2 : 1: 1	39%
43	CaO-Dolomite[m] (3.57 mmol/g)	20 mol%	EtOH/4	80/4	2 : 1: 1	36%
44	CaO	10 mol%	EtOH/4	80/4	2 : 1: 1	31%
45	SnO_2	10 mol%	EtOH/4	80/4	2 : 1: 1	36%
46	MK30[n]	0.3 g	EtOH/4	80/4	2 : 1: 1	43%

[a] Unless stated otherwise, reactions were performed on a 2.5 mmol scale using a molar ratio of 2 (salicylaldehyde): 1 (malononitrile): 1 (morpholine) in a stepwise fashion i.e. aldehyde and malononitrile were mixed along with catalyst and a few drops of solvent for 10–15 min at room temperature before adding amine and further ethanol and then heating. Other trials involved mixing aldehyde, malononitrile, solvent and catalyst and then adding the amine immediately after.
[b] Yield of pure isolated product confirmed by ^{1}H NMR, IR, MS, ^{13}C NMR. Product was purified by dissolving in acetone, drying and then recrystallizing from ethanol.
[c] Catalyst was crushed with hammer and ground using pestle and mortar.
[d] Chlorosulfonic acid treated silica-bonded CPTMS-DABCO (method in experimental section).
[e] DBU supported on Amberlyst® 15.
[f] Silica-bonded CPTMS-Piperazine (method in experimental section).
[g] Ethylenediamine supported on Amberlyst® 15(method in experimental section).
[h] Methane sulfonic acid supported on alumina (method in experimental section).
[i] 40% w/w silicotungstic acid supported on alumina (method in experimental section).
[j] 25% w/w silicotungstic acid supported on Amberlyst® 15.
[k] 20% w/w sulfated zirconia (method in experimental section).
[l] 20% w/w sulfated alumina (method in experimental section).
[m] Calcium oxide supported on dolomite (method in experimental section).
[n] Montmorillonite K30.

The latter phenomenon (lower yields) could be explained either in terms of chromeno[2,3-*b*]pyridine side product formation (catalysed by the amine itself) or the formation of other side products; one of which was fluorescent (not isolated) and the other being caused by the reaction of the solvent (methanol) instead of the amine (^{1}H NMR spectrum of the isolated side product in Supplementary Information). In fact, the latter reaction was significantly pronounced when the amine used was dibutylamine (Table 7**, entry 4**) whose reactivity obviously suffered from classical steric hindrance.

3.4. Catalyst recycling runs

The catalyst **Pip-A15-A** could be recycled and reused for all three reactions. The synthesis of the 4*H*-chromenes provided consistently good yields (Fig. 4) for the combination of malononitrile (**1a**), salicylaldehyde (**2a**) and 2-methylindole (**4a**) after 5 consecutive runs even if the reaction time had to be increased slightly from the 1st round to the 2nd round. [Note that this reaction was chosen to conduct the recycling runs owing to the fact that the product could be collected easily by recrystallization instead of column chromatography (more solvent use)]. The latter was probably because of the fact that one of the starting materials or the product (**9b-i**) itself got adsorbed onto the catalyst surface as could be understood from the change in colour. An attempt at reusing catalyst **Pip-A15-B** for the synthesis of **9b-I** at the conditions of Table 2**, entry 18** gave a similar pattern to that of **Pip-A15-A** albeit all runs had to be conducted for longer (10 h) and using double the molar equivalent (Fig. 5).

Meanwhile, in the synthesis of the model chromeno[2,3-*b*]pyridine **10a**, the yield decreased slightly from the 1st to the 2nd round but then remained practically the same. This further proves that the catalyst is getting "poisoned" mostly during the 1st cycle. Lastly, for the synthesis of the chromeno[2,3-*d*]pyrimidine **12a**, the yield decrease was more gradual but the reaction time had to be increased by a factor of two from the 1st run to the 2nd one (Fig. 4).

A hot filtration test on the model reaction for the synthesis of product **9b-i** using catalyst **Pip-A15-A** was conducted, and confirmed that the leaching was minimal because once removed from the reaction mixture, the latter stopped proceeding. From the recycling runs and from the hot filtration test it can be stated that even if **Pip-A15-A** probably consisted of some piperazine which was trapped within the polymeric matrix but was not covalently bonded per se, physisorption forces were enough to minimise leaching rendering the catalytic process heterogeneous. The low temperature utilised helped in this regard as well.

3.5. Spectral analysis of model reaction product 9b-i

3.5.1. IR spectrum (see Supporting information)

In the IR spectrum of the 4-indolyl-4*H*-chromene **9b-i** the small band at 3445 cm^{-1} is contributed by the indole N–H stretch whilst the wider one at 3343 cm^{-1} probably houses both asymmetric and symmetric amine NH_2 stretches. Bands at 3196 cm^{-1} and 3167 cm^{-1} are probably overtone bands of the indolyl and amino N–H bending modes. The strong narrow band at 2189 cm^{-1} is the result of nitrile stretching. In between 1651 cm^{-1} and 1456 cm^{-1} there are aromatic C–H stretching modes as well as the amine N–H bending mode (possibly the one at 1651 cm^{-1}). C–N stretching is exhibited at 1261 cm^{-1}. Close by at 1227 cm^{-1}, there is the C–O stretch whilst further to the right, from 1184 to 1015 cm^{-1} there are the in-plane aromatic C–H bending modes. In the region 768–669 cm^{-1} there are the complementary out-of-plane bending modes as well as the NH wagging band (should be the one at 768 cm^{-1}).

3.5.2. ^{1}H NMR spectrum (see Supporting information)

A series of proton-decoupling experiments (see Supporting information) helped in the assignment of the aromatic hydrogens in the ^{1}H NMR spectrum of **9b-i**. The peak with the highest chemical shift (at 9.96 ppm) belongs to H17 owing to the negative inductive effects of the nitrogen atom and the electron-sharing to generate aromaticity.

The two doublets at 7.27 and 7.15 ppm are possibly due to H19 and H21 respectively. Moving on to the chromene moiety, the *ddd* at 7.21 ppm should be due to H6 which is *meta* to the oxygen (i.e. not electron-rich) and has a common coupling constant with H3 (a *dd* at 7.07 ppm) of 1.2 Hz. Then, the multiplet at 7.03–6.94 ppm is considered a result of hydrogens H4,5 and 20 and the *ddd* at 6.82 ppm (J = 8.0, 7.0, 1.0 Hz) is due to H22. The characteristic singlet at 5.99 ppm is created by H13. H10 is visible at 5.07 ppm and the methyl hydrogens (H23) give rise to singlet at 2.45 ppm.

Table 5
Expansion of substrate scope for the synthesis of 4*H*-chromene derivatives (**9a-e**) using Pip-A15-A catalyst

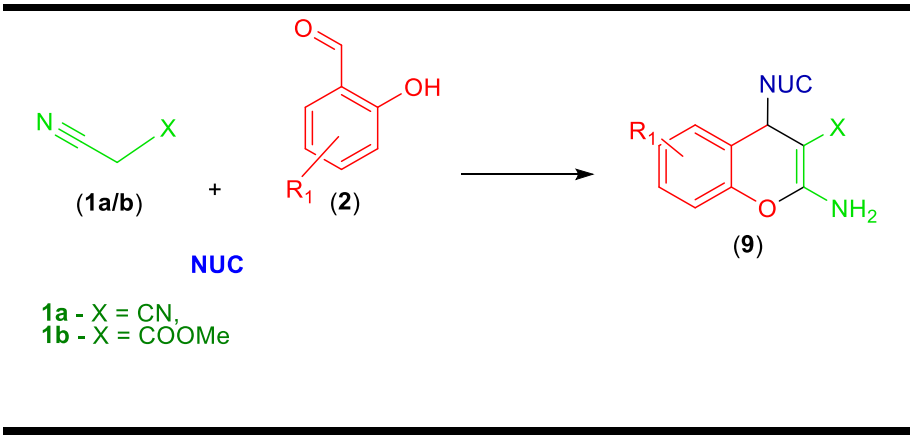

Entry[a]	R^1 (reactant code)	1a/b	NUC	Temperature [°C] / Time (hrs)	Yield (%)[b]	E-factor[c]
1 (model)	H **(2a)**	CN **(1a)**	Ph-SH **(3a)**	50 / 8	82%[d] **(9a-i)**	5.79
2	5-Br **(2b)**	CN **(1a)**	Ph-SH **(3a)**	50 / 4	70% **(9a-ii)**	5.52
3	4-OH **(2c)**	CN **(1a)**	Ph-SH **(3a)**	50 / 4 80 / 4	0% 0% **(9a-iii)**	-
4	5-NO_2 **(2d)**	CN **(1a)**	Ph-SH **(3a)**	50 / 4	70% **(9a-iv)**	6.05
5	**5-NO_2 (2d)**	**CN (1a)**	**4-Me-Ph-SH (3b)**	**80 / 4**	**73% (9a-v)**	**5.54**
6	H **(2a)**	CN **(1a)**	2-MeIndole **(4a)**	50 / 5	82% **(9b-i)**	5.4
7	H **(2a)**	CN **(1a)**	Indole **(4b)**	50 / 6	75%[d] **(9b-ii)**	6.28
8	5-Br **(2b)**	CN **(1a)**	2-MeIndole **(4a)**	50 / 5	54% **(9b-iii)**	7.09
9	4-OH **(2c)**	CN **(1a)**	2-MeIndole **(4a)**	50 / 4 80 / 4	0% 0% **(9b-iv)**	-
10	**5-Cl (2e)**	**CN (1a)**	**5-BrIndole (4c)**	**50 / 4 80 / 4**	**- 57% (9b-v)**	**6.36**
11	H **(2a)**	CN **(1a)**	$MeNO_2$ **(5)**	50 / 4	61%[d] **(9c-i)**	9.72
12	5-Br **(2b)**	CN **(1a)**	$MeNO_2$ **(5)**	50 / 4	45% **(9c-ii)**	10.40
13[f]	H **(2a)**	CN **(1a)**	2-Naphthol **(6)**	50 / 14	15% **(9d-i)**	32.84
14[e]	H **(2a)**	CN **(1a)**	NH_2NH_2 **(8)** + EtAcOAc **(9)**	50 / 4	35% **(9e-i)**	15.51
15	H **(2a)**	COOMe **(1b)**	$MeNO_2$ **(5)**	50 / 6	71% **(9c-iii)**	7.24
16	**5-Br (2b)**	**COOMe (1b)**	**$MeNO_2$ (5)**	**50 / 6**	**74% (9c-iv)**	**5.40**
17	**5-Cl (2e)**	**COOMe (1b)**	**$MeNO_2$ (5)**	**50 / 6**	**67% (9c-v)**	**6.89**
18	**H (2a)**	**COOMe (1b)**	**2-MeIndole (4a)**	**50 / 6**	**18% (9b-vi)**	**25.84**

[a] = Reaction performed in the presence of 10 mol% Pip-A15-A in 4 mL ethanol using a molar ratio of reactants of 1 : 1 : 1 at a 2.5 mmol scale;
[b] Yield of pure product collected after recrystallization from ethanol unless otherwise stated;
[c] *E-factor* = total mass of waste (including ethanol solvent added during reaction) / total mass of product;
[d] Yield of pure product collected after column chromatography;
[e] During this trial after the addition of malononitrile, salicylaldehyde, the catalyst and the solvent, hydrazine and ethyl acetoacetate were added due to the latter's reaction to form a nucleophilic substrate;
[f] Reaction performed under nitrogen

3.5.3. ^{13}C NMR spectrum (see Supporting information)

The most deshielded carbon is likely to be C14 because it is adjacent to two electronegative atoms (O and N). The peak due to the latter carbon is absent on the DEPT spectrum. Slightly upfield, at 149.57 ppm there is a peak (also absent on DEPT) that could be due to C15 since it is adjacent to the electronegative oxygen and is part of the aromatic ring. Since N is less

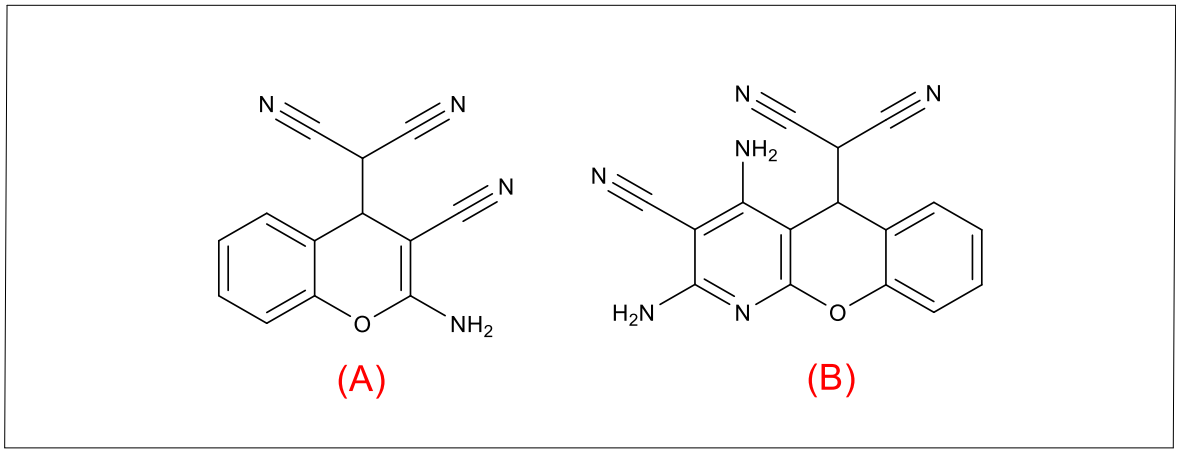

Fig. 3. Side products which formed during the synthesis of 4*H*-chromenes (**9**).

Table 6
Expansion of substrate scope in the synthesis of chromeno[2,3-*b*]pyridines (**10a-h**)

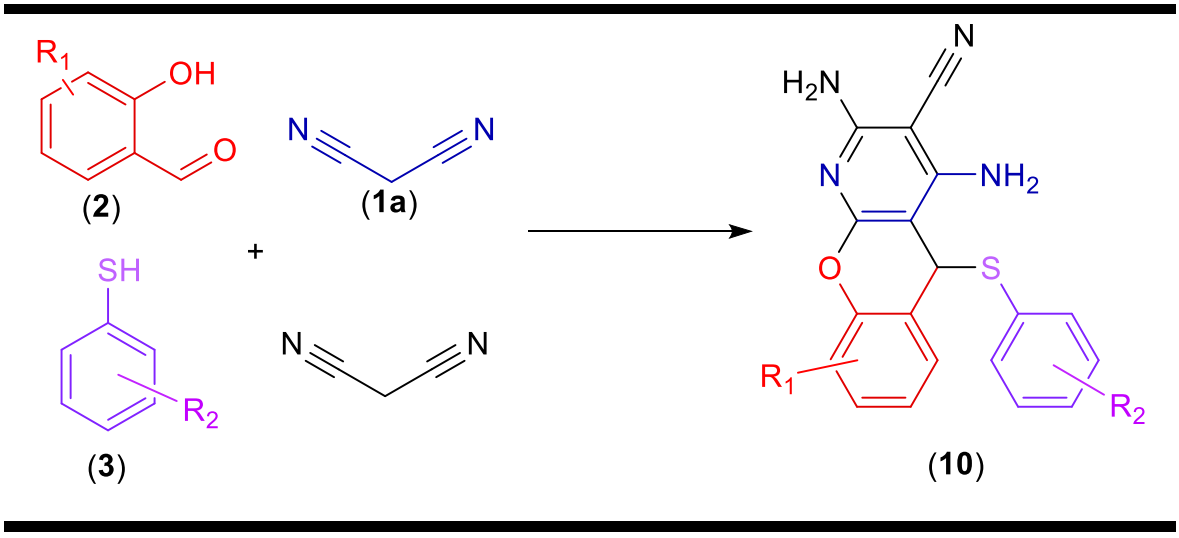

Entry[a]	R^1	R^2	Time (hrs)	Yield (%)[b]	E-factor[c]
1 (model)	H (**2a**)	H (**3a**)	4	75% (**10a**)	5.6
2[d]	5-Br (**2b**)	H (**3a**)	12	40% (**10b**)	9.5
3[d]	5-NO_2 (**2d**)	H (**3a**)	4	63% (**1°C**)	6.1
4[d]	5-Cl (**2e**)	H (**3a**)	12	38% (**10d**)	11.1
5[d]	H (**2a**)	4-Me (**3b**)	8	57% (**10e**)	7.4
6	H (**2a**)	4-Br (**3c**)	4	62% (**10f**)	5.8
7[d]	**5-NO_2** (**2d**)	**4-Br** (**3c**)	**8**	**17%** (**10g**)	**21.8**
8[d]	5-NO_2 (**2d**)	4-Me (**3b**)	8	34% (**10h**)	11.8

[a] = Reaction performed in the presence of 10 mol% Pip-A15-A in 4 mL ethanol using a molar ratio of reactants (1a/2/3) of 1 : 1 : 2 at a 2.5 mmol scale at 80°C ;
[b] Yield of pure product collected after addition of water to filtered crude mixture dissolved in DMF;
[c] *E-factor* = total mass of waste (including ethanol solvent used during reaction) / total mass of product;
[d] Yield of pure product collected after addition of water to crude mixture dissolved in DMF followed by recrystallization from methanol

electronegative than O, it follows that the peak at 135.99 ppm belongs to C2 while that at 132.21 ppm to C8 (both peaks absent on DEPT). Based on the order of peaks in the ^{1}H NMR spectrum, the peaks at 129.54, 127.76, 124.46, 120.41 ppm (all visible on DEPT) are probably caused by carbons C3, C20, C4 and C17 respectively. Meanwhile, C1 (absent on DEPT) should be that at 127.13 ppm considering its proximity to the nitrogen and C13 (also absent on DEPT) that at 123.00 ppm. The latter is rendered electron-rich compared to C1 because of the positive

Table 7
Expansion of substrate scope for the synthesis of chromeno[2,3-*d*]pyrimidine (**12a- h**)

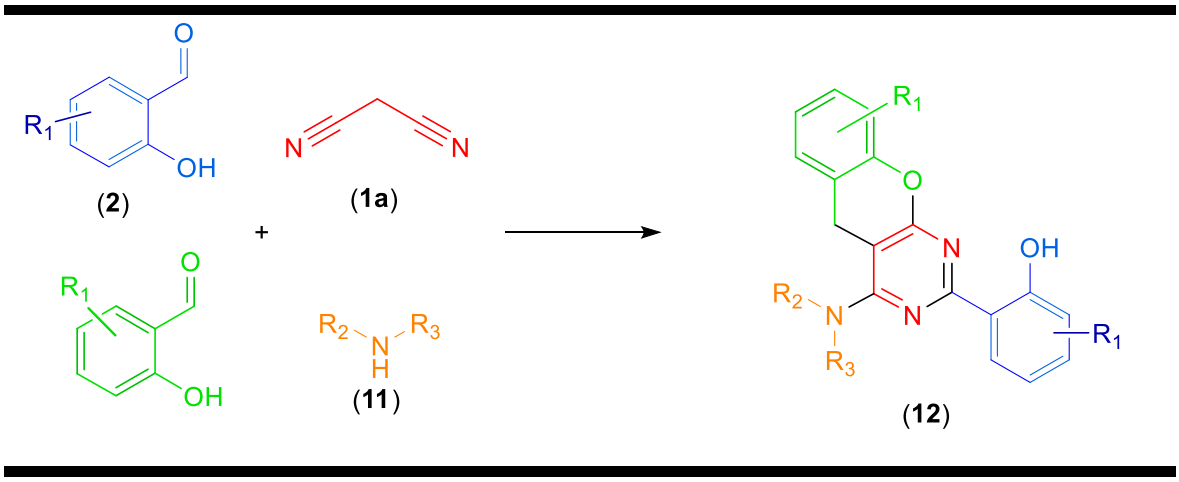

Entry[a]	R^1 (reactant code)	R^2, R^3 (reactant code)	Time (hrs)	Yield (%)[b] (product code)	*E*-factor
1 (model)	H **(2a)**	$-CH_2CH_2OCH_2CH_2-$ **(11a)**	4	70% **(12a)**	5.42
2	H **(2a)**	$-CH_2CH_2CH_2CH_2CH_2-$ **(11b)**	4	68% **(12b)**	5.64
3	H **(2a)**	$-CH_2CH_2CH_2CH_2-$ **(11c)**	4	23% **(12c)**	19.24
4[c]	**H (2a)**	***n*-Bu- (11d)**	**5**	**10% (12d)**	**40.28**
5	H **(2a)**	Et- **(11e)**	5	10% **(12e)**	45.31
6	5-Br **(2b)**	$-CH_2CH_2OCH_2CH_2-$ **(11a)**	5	52% **(12f)**	5.60
7	5-Br **(2b)**	$-CH_2CH_2CH_2CH_2CH_2-$ **(11b)**	5	46% **(12g)**	7.55
ss8	5-Cl **(2e)**	$-CH_2CH_2OCH_2CH_2-$ **(11a)**	5	40%[d] **(12h)**	6.02
9	5-Cl **(2e)**	$-CH_2CH_2CH_2CH_2CH_2-$ **(11b)**	5	40%[d] **(12i)**	6.00
10	5-NO_2 **(2d)**	$-CH_2CH_2OCH_2CH_2-$ **(11a)**	5	0% **(12j)**	-
11	5-NO_2 **(2d)**	$-CH_2CH_2CH_2CH_2CH_2-$ **(11b)**	5	0% **(12k)**	-

[a] = Reaction performed in the presence of 10 mol% Pip-A15-A in 4 mL methanol using a molar ratio of reactants (1a/2/11) of 1 : 1 : 2 at a 2.5 mmol scale at 70°C ;
[b] Yield of pure product collected after recrystallization from ethanol;
[c] Yield of pure product collected after column chromatography using 9:1 hexane/ethyl acetate
[d] Products had to be recrystallized first from ethanol and then from methanol

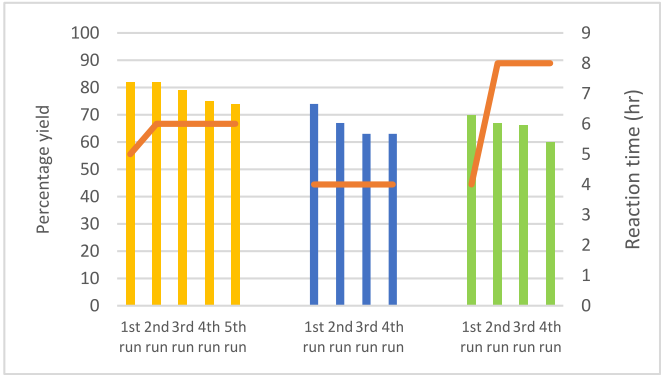

Fig. 4. Recycling runs for the synthesis of 4*H*-chromene **9b-i (yellow bars)**, the chromeno[2,3-*b*]pyridine **10a (blue bars)** and the chromeno[2,3-*d*]pyrimidine **12a (green bars)** using **Pip-A15-A**. Orange line represents reaction time (hours). (For interpretation of the references to colour in this figure legend, the reader is referred to the Web version of this article.)

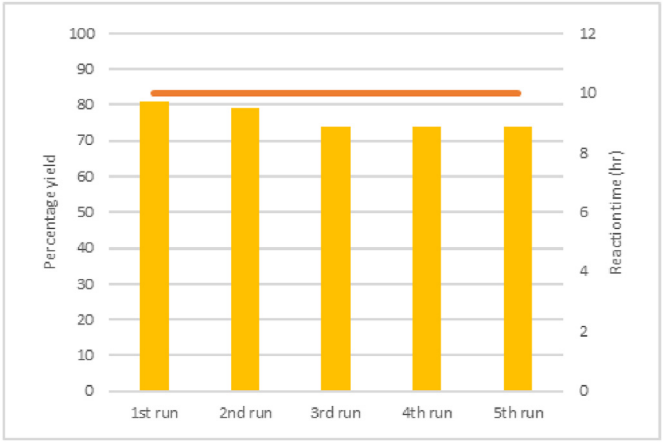

Fig. 5. Recycling runs for the synthesis of 9b-i using Pip-A15-B. Orange line represents reaction time (hours). (For interpretation of the references to colour in this figure legend, the reader is referred to the Web version of this article.)

mesomeric effect exerted by O. Moving towards lower chemical shifts, C21 (absent on DEPT) is likely to be that at 119.63 ppm whereas C7 (also absent on DEPT) should be that at 114.25 ppm. In this case, the assignment was based on the reasoning that C7 is the most electron-rich atom of indole whereas C21, although *sp* hybridized, is bonded directly to N (hence comparatively rendered electron-poor by negative inductive effect). C18 and C19 could be the peaks at 118.61 and 117.89 ppm respectively. Thereafter, C5 and C6 (both visible in DEPT) are at 115.75 and 110.52 ppm respectively. C12, absent on DEPT, should be the peak at 58.67 ppm because it is rendered electron-rich by the positive mesomeric effect exerted by the amino group. The aliphatic carbons C11 and C10 (present in DEPT) appear at 31.42 and 10.77 ppm respectively.

4. Conclusion

Piperazine supported on Amberlyst® 15 (Pip-A15) was found to be a relatively economic, easy to synthesize novel green catalyst. It was able to catalyse the synthesis of 2-amino-4*H*-chromenes (18 products, 5 of which were novel) derived from salicylaldehyde, malononitrile/methyl cyanoacetate and a range of nucleophilic species (thiophenols, naphthol, indoles, nitromethane and hydrazine/ethyl acetoacetate). Simultaneously, the same catalyst was found to be suitable (amongst the wide range which was screened) in the synthesis of chromeno[2,3-*b*]pyridines and chromeno[2,3-*d*]pyrimidines (8 + 8 products, 2 of which were novel). Most importantly the catalyst was also characterised, titrated (for alkalinity determination) and could be recycled and reused. To the best of our knowledge, there has not yet been any similar study whereby the same catalyst could be used for the synthesis of all three types of chromenes. Ethanol was the only solvent used both for the preparation of the catalyst and for all reactions.

Declaration of competing interest

The authors declare that they have no known competing financial interests or personal relationships that could have appeared to influence the work reported in this paper.

Acknowledgements

The authors thank the University of Malta for financial and technical support. The authors would also like to thank Dr. Duncan Micallef for assistance with the acquisition of the NMR spectra, and Dr. Godwin Sammut for MS analyses.

Appendix A. Supplementary data

Supplementary data to this article can be found online at https://doi.org/10.1016/j.tgchem.2023.100011.

References

[1] P. Roudini, N. Hazeri, H.F. Niya, H.F. Fatahpour, Fe_3O_4@THAM-SO_3H: an eco-friendly solid acid nanocatalyst for synthesis of 2-amino-3-cyanopyridines and 2,4,6-triarylpyridines under mild reaction conditions, Polycycl. Aromat. Comp. 42 (2022) 1–16.

[2] F. Sameri, M.A. Bodaghifard, A. Mobinkhaledi, Ionic-liquid-coated nanoparticles (CaO@SiO_2@BAIL): a bi-functional and environmentally benign catalyst for green synthesis of pyridine, pyrimidine and pyrazoline derivatives, Polycycl. Aromat. Comp. 42 (7) (2022) 4700–4716.

[3] S. Swami, A. Agarwala, R. Shrivastava, Sulfonic acid functionalized silica-coated $CuFe_2O_4$ core–shell nanoparticles: an efficient and magnetically separable heterogeneous catalyst for the synthesis of 2-pyrazole-3-amino-imidazo-fused polyheterocycles, New J. Chem. 40 (11) (2016) 9788–9794.

[4] M.S.A. El-Gaby, M.A. Zahran, M.M.F. Ismail, Y.A. Ahmmar, A novel synthesis of dibenzo[*c,f*]chromenes, dibenzo[*c,h*]chromenes and benzo[7,8]chromeno[3,4-*f*] isoindoles as antimicrobial agents, Il Farmaco 55 (2000) 227–232.

[5] M. Vosooghi, S. Rajabalian, M. Sorkhi, M. Badinloo, M. Nakhjiri, A.S. Negahbani, A. Asadipour, M. Mahdavi, A. Shafiee, A. Foroumadi, Synthesis and cytotoxic activity of some 2-amino-4-aryl-3-cyano-7-(dimethylamino)-4*H*-chromenes, Res. Pharm. Sci. 5 (2010) 9–14.

[6] S.A. Patil, J. Wang, X.S. Li, J. Chen, T.S. Jones, A. Hosni-Ahmed, R. Patil, W.L. Seibel, W. Li, D.D. Miller, New substituted 4*H*-chromenes as anticancer agents, Bioorg. Med. Chem. Lett. 22 (2012) 4458–4461.

[7] H. Zhu, G. Xu, H. Du, C. Zhang, N. Ma, W. Zhang, Prolinamide functionalized polyacrylonitrile fiber with tunable linker length and surface microenvironment as efficient catalyst for Knoevenagel condensation and related multicomponent tandem reactions, J. Catal. 374 (2019) 217–229.

[8] A.R. Kiasat, S. Hamid, S.J. Saghanezhad, Bipyridinium chloride supported rice husk silica: an efficient nanocomposite for the one-pot preparation of spirooxindole pyran and 2-amino-4*H* chromene derivatives, Rev. Roum. Chem. 64 (2019) 927–934.

[9] A. Neela, T. Clarina, V. Rama, Nickel oxide-catalyzed synthesis of 4-amino-2*H*-chromenes: its application in antimicrobial studies and towards protein docking, Chem. Asian J. 31 (2019) 1049–1056.

[10] A. Khazee, R. Jahanshahi, S. Sobhani, J. Skibsted, J.M. Sansano, Immobilized piperazine on the surface of graphene oxide as a heterogeneous bifunctional acid-base catalyst for the multicomponent synthesis of 2-amino-3-cyano-4H-chromenes, Green Chem. 22 (2020) 4604–4616.

[11] N. Azizi, M. Mariami, M. Edrisi, Greener construction of 4*H*-chromenes based dyes in deep eutectic solvent, Dyes Pigments 100 (2014) 215–221.

[12] A.K. Gupta, K. Kumari, N. Singh, S. Raghuvanshim, K.N. Singh, An eco-safe approach to benzopyranopyrimidines and 4*H*-chromenes in ionic liquid at room temperature, Tetrahedron Lett. 53 (2012) 650–653.

[13] S.M. Sadeghzadeh, M.A. Nasseri, PbS nanoparticles stabilized on HPG-modified $FeNi_3$ as catalyst for synthesis of 2-amino-4*H*-chromene under mild conditions, J. Iran. Chem. Soc. 11 (2013) 1197–1205.

[14] K. Kantharaju, S.Y. Khatavi, A green method synthesis and antimicrobial activity of 2-amino-4*H*-chromenes, Asian J. Chem. 30 (2018) 1496–1502.

[15] G.S. Nongthombam, R. Nongkhlaw, Experimental and theoretical studies on SPION@glutathione catalyzed synthesis of indolyl chromene, indolo xanthene, and pyrimido[4,5-*b*]quinoline, Synth. Commun. 48 (2018) 541–552.

[16] P.P. Ghosh, A.R. Das, Nanocrystalline and reusable ZnO Catalyst for the assembly of densely functionalized 4*H*-chromenes in aqueous medium via one-pot three component reactions: a greener "NOSE" approach, J. Org. Chem. 78 (2013) 6170–6181.

[17] N.V. Lakshmi, S.E. Kiruthika, P.T. Perumal, A rapid and efficient access to 4-substituted-2-amino-4*H*-chromenes catalysed by $InCl_3$, Synlett 10 (2011) 1389–1394.

[18] M. Kidwai, R. Chauhan, K_2CO_3 catalyzed green and rapid access to 2-amino-3,5-dicarbonitrile-6-thio-pyridines, J. Iran. Chem. Soc. 11 (2014) 1005–1013.

[19] J. Safei-Ghomi, M. Kiani, A. Ziarati, H. Shahbazi-Alavi, Highly efficient synthesis of benzopyranopyridines via ZrP_2O_7 nanoparticles catalyzed multicomponent reactions of salicylaldehydes with malononitrile and thiols, J. Sulphur Chem. 35 (2014) 450–457.

[20] J. Safaei-Ghomi, H. Shahbazi-Alavi, E. Heidari-Baghbahadorani, SnO nanoparticles as an efficient catalyst for the one-pot synthesis of chromeno[2,3-*b*]pyridines and 2-amino-3,5-dicyano-6-sulfanyl pyridines, RSC Adv. 4 (2014) 50668–50677.

[21] J. Safaei-Ghomi, M. Tavazo, M.R. Vakili, H. Shahbazi-Alavi, Chitosan functionalized by citric acid: an efficient catalyst for one-pot synthesis of 2,4-diamino-5*H*-benzopyrano[2,3-*b*]pyridine-3-carbonitriles 5-(arylthio) or 5-[(arylmethyl)thio] substituted, J. Sulphur Chem. 38 (2017) 236–248.

[22] H.R. Shaterian, M. Aghakhanizadeh, Aminopropyl coated on magnetic Fe_3O_4 and SBA-15 nanoparticles catalyzed mild preparation of chromeno[2,3-*d*]pyrimidines under ambient and solvent-free conditions, Catal. Sci. Technol. 3 (2013) 425–428.

[23] S.M. Sadeghzadeh, F. Daneshfar, M. Malekzadeh, Manganese(III) salen complex immobilized on Fe_3O_4 magnetic nanoparticles: the efficient, green and reusable nanocatalyst, Chin. J. Chem. 32 (2014) 349–355.

[24] B. Umamahesh, T.R. Mandlimath, K.I. Sathiyanarayanan, A novel, facile, rapid, solvent free protocol for the one pot green synthesis of chromeno[2,3-*d*]pyrimidines using reusable nano $ZnAl_2O_4$-NOSE approach and their photophysical studies, RSC Adv. 5 (2015) 6578–6587.

[25] B. Thirupathaiah, M.V. Reddy, Y.T. Jeong, Solvent-free sonochemical multi-component synthesis of benzopyranopyrimidines catalyzed by polystyrene supported *p*-toluenesulfonic acid, Tetrahedron 71 (2015) 2168–2176.

[26] M.J. Nasab, A.R. Kiasat, Covalently anchored 2-amino ethyl-3-propyl imidazolium bromide on SBA-15 as a green, efficient and reusable Brønsted basic ionic liquid nanocatalyst for one-pot solvent-free synthesis of benzopyranopyrimidines under ultrasonic irradiation, RSC Adv. 92 (2015) 75491–75499.

[27] S. Sadjadi, M.M. Heravi, M. Malmir, Heteropolyacid@creatin-halloysite clay: an environmentally friendly, reusable and heterogeneous catalyst for the synthesis of benzopyranopyrimidines, Res. Chem. Intermed. 43 (2017) 6701–6717.

[28] G. Kour, M. Gupta, A nano silver-xerogel (Agnps@modifiedTEOS) as a newly developed nanocatalyst in the synthesis of benzopyranopyrimidines (with secondary and primary amines) and gem-bisamides, Dalton Trans. 46 (2017) 7039–7050.

[29] S.A. Kabeer, G.R. Reddy, P. Sreelakshmi, D.M. Manidhar, C.S. Reddy, TiO_2-SiO_2 catalyzed eco-friendly synthesis and antioxidant activity of benzopyrano[2,3-*d*] pyrimidine derivatives, J. Heterocycl. Chem. 54 (2017) 2598–2604.

[30] M.M. Mostafavi, F. Movahedi, Synthesis, characterization, and heterogeneous catalytic activity of sulfamic acid functionalized magnetic IRMOF-3, Eur. J. Inorg. Chem. 2019 (2019) 787–793.

[31] F.M. Moghaddam, N. Masoud, K. Foroushani, S. Saryazdi, N. Ghonouei, E. Daemi, Silica-supported DABCO-tribromide: a recoverable reagent for oxidation of alcohols to the corresponding carbonyl compounds, Sci. Iran. 20 (2013) 598–602.

[32] X. Zhang, S. Liu, Y. Gao, Y. Zhang, L. Ren, R. Huand, R. Chen, Preparation of amine functionalized porous silica by ultrasonic technique for the methylation reaction of phenol with dimethyl carbonate, J. Chem. Soc. Pakistan 35 (2013) 1284–1287.
[33] B. Sutrisno, A.D. Nafiah, I.S. Fauziah, W. Kurniawan, H. Hinode, A. Hidayat, CaO/Natural Dolomite as a heterogeneous catalyst for biodiesel production, Mater. Sci. Forum 991 (2019) 117–122.
[34] E.J. Lenardao, P.C. Ferreira, R.G. Jacob, G. Perin, F.P.L. Leite, Solvent-free conjugated addition of thiols to citral using KF/alumina: preparation of 3-thioorganyylcitronellas, potential antimicrobial agents, Tetrahedron Lett. 48 (2007) 6763–6766.
[35] J. Balou, M.A. Khalilzadeh, D. Zareyee, An efficient and reusable nano catalyst for the synthesis of benzoxanthene and chromene derivatives, Sci. Rep. 9 (2019) 3605–3613.
[36] S.L. Daisy, A.C.C. Mary, K. Devi, S.S. Prabha, S. Rajendran, S.S. Zahirullah, Magnesium oxide nanoparticles – synthesis and characterisation, Int. J. Nano Corr. Sci. Eng. 2 (2015) 64–69.
[37] C.S. Maheswari, C. Shanmugapriya, K. Revathy, A. Lalitha, SnO_2 nanoparticles as an efficient heterogeneous catalyst for the synthesis of 2*H*-indazolo[2,1-*b*]phthalazine-triones, J. Nanostr. Chem. 7 (2017) 283–291.
[38] L. Habte, N. Shiferaw, D. Mulatu, T. Thenepalli, R. Chilakala, J.W. Ahn, Synthesis of nano-calcium oxide from waste eggshell by sol-gel method, Sustainability 11 (2019) 3196–3205.
[39] M. Vakili, P. Amouzgar, G. Cagnetta, B. Wang, X. Guo, A. Mojiri, E. Zeimaran, B. Salamatinia, Ultrasound-assisted preparation of chitosan/nano-activated carbon composite beads aminated with (3-aminopropyl)triethoxysilane for adsorption of acetaminophen from aqueous solutions, Polymers 11 (2019) 1701–1712.
[40] M.V. Lombardo, M. Videla, A. Calvo, F.G. Requejo, G.J.A.A. Soler-Illia, Aminopropyl-modified mesoporous silica SBA-15 as recovery agents of Cu(II) sulfate solutions: adsorption efficiency, functional stability and reusability aspects, J. Hazard Mater. 223 (2012) 53–62.
[41] I. Lukic, J. Krstic, D. Jovanovic, D. Skala, Alumina/silica supported K_2CO_3 as a catalyst for biodiesel synthesis from sunflower oil, Bioresour. Technol. 100 (2009) 4690–4696.
[42] M. Fan, P. Zhang, Q. Ma, Enhancement of biodiesel synthesis from soybean oil by potassium fluoride modification of a calcium magnesium oxides catalyst, Bioresour. Technol. 104 (2012) 447–450.
[43] H. Sharghi, M. Jokar, Highly stereoselective facile synthesis of β-amino carbonyl compounds via a Mannich-type reaction catalyzed by γ-Al_2O_3/$MeSO_3H$ (alumina/methanesulfonic acid: AMA) as a recyclable, efficient, and versatile heterogeneous catalyst, Can. J. Chem. 88 (2009) 14–26.
[44] S. Zhu, Y. Zhu, X. Gao, T. Mo, Y. Zhu, Y. Li, Production of bioadditives from glycerol esterification over zirconia supported heteropolyacids, Bioresour. Technol. 130 (2013) 45, 41.
[45] M. Shekouhy, R. Kordnezhadian, A. Khalafi-Nezhad, Silica-bonded DABCO hydrogen sulfate ((SB-DABCO)HSO_4): a new dualinterphase catalyst for the diversity-oriented pseudo-five-component synthesis of bis(pyrazolyl)methanes and novel 4-[bis(pyrazolyl)methane]phenylmethylene-bis(indole)s, J. Iran. Chem. Soc. 15 (2018) 2357–2368.
[46] M. Keshavarz, N. Iravani, A. Ghaedi, A.Z. Ahmady, M. Vafaei-Nezhad, S. Karimi, Macroporous polymer supported azide and nanocopper (I): efficient and reusable reagent and catalyst for multicomponent click synthesis of 1,4-disubstituted-1H-1,2,3-triazoles from benzyl halides, SpringerPlus 2 (2013) 1–8.
[47] A. Khalafi, M. Nourisefat, F. Panahi, L-Cysteine functionalized magnetic nanoparticles (LCMNP): a novel magnetically separable organocatalyst for one-pot synthesis of 2-amino-4*H*-chromene-3-carbonitriles in water, Org. Biomol. 13 (2015) 7772–7779.
[48] S.K. Shinde, M.T. Patil, S.A. Damate, S.S. Patil, Synergetic effects of naturally sourced metal oxides in organic synthesis: a greener approach for the synthesis of pyrano[2,3-*c*]pyrazoles and pyrazolyl-4*H*-chromenes, Res. Chem. Intermed. 44 (2018) 1775–1795.
[49] P.G. Patil, S. Sehlangia, D.H. More, Chitosan-SO_3H (CTSA) an efficient and biodegradable polymeric catalyst for the synthesis of 4,4′-(arylmethylene)bis(1*H*-pyrazol-5-ol) and α-amidoalkyl-β-naphthol's, Synth. Commun. 50 (2020) 1696–1711.
[50] S. Mishra, R. Ghosh, K_2CO_3-mediated, one-pot, multicomponent synthesis of medicinally potent pyridine and chromeno[2,3-*b*]pyridine scaffolds, Synth. Commun. 41 (2011) 2229–2244.
[51] H. Gan, W. Cao, Z. Fang, X. Li, S. Tang, K. Guo, Efficient synthesis of chromenopyridine and chromene via MCRs, Chin. Chem. Lett. 25 (2014) 1357–1362.
[52] W.W. Sulkowski, K. Nowak, A. Sulkowska, B. Mikula, W.M. Bajdur, D. Pentak, A. Wolinska, Study of the sulfonation of expanded polystyrene waste and of properties of the products obtained, Pure Appl. Chem. 81 (2009) 2417–2424.